NATIONAL ADVISORY COMMITTEE FOR AERONAUTICS

WARTIME REPORT

ORIGINALLY ISSUED

June 1944 as
Advance Restricted Report 4F17

A COMPARISON OF THE EFFECTS OF FOUR-BLADE DUAL- AND SINGLE-ROTATION PROPELLERS ON THE STABILITY AND CONTROL CHARACTERISTICS OF A HIGH-POWERED SINGLE-ENGINE AIRPLANE

By Charles W. Harper and Bradford H. Wick

Ames Aeronautical Laboratory
Moffett Field, California

NACA

WASHINGTON

NACA ARR No. 4F17

NATIONAL ADVISORY COMMITTEE FOR AERONAUTICS

ADVANCE RESTRICTED REPORT

A COMPARISON OF THE EFFECTS OF FOUR-BLADE DUAL- AND SINGLE-ROTATION PROPELLERS ON THE STABILITY AND CONTROL CHARACTERISTICS OF A HIGH-POWERED SINGLE-ENGINE AIRPLANE

By Charles W. Harper and Bradford H. Wick

SUMMARY

A 3/16-scale powered model of the Douglas XSB2D-1 airplane was tested with a four-blade dual-rotation propeller and a four-blade single-rotation propeller. To make the results more directly comparable, no other changes were made to the model. The characteristics of the model were determined for a number of different operating conditions for each type of propeller. The differences in characteristics are examined, and explanations are advanced where possible. Although the results are directly applicable only to the XSB2D-1 model, it is felt that they are indicative of what might be expected from a similar change in propeller type on any other high-powered single-engine airplane.

The longitudinal stability of the model was found to be somewhat less with the dual-rotation propeller than with the single-rotation propeller. This was due partially to an increase in the destabilizing propeller forces and partially to an increase in the extent of the tail immersed in the slipstream and the attendant destabilizing effects.

The directional characteristics were most affected by the change in propeller type. The differences between the characteristics in yaw with a dual-rotation and with a single-rotation propeller installed are shown to be almost wholly due to the rotation of the resulting slipstream. From results of tests with the single-rotation

propeller installed, the available yaw range was found to be asymmetrically disposed about zero yaw and a significant yawing moment was found to exist at zero yaw at all but the lowest power condition. From results of tests with the dual-rotation propeller installed, the available yaw range, while not significantly changed in magnitude, was found to be symmetrically disposed about zero yaw, and zero yawing moment was found to exist at zero yaw for all power conditions.

No difference of any consequence was found between the lateral characteristics of the model when tested with a dual-rotation propeller and when tested with a single-rotation propeller.

INTRODUCTION

Tests of a 3/16-scale powered model of the Douglas XSB2D-1 airplane with a four-blade single-rotation propeller revealed a number of characteristics considered undersirable from a flying-qualities standpoint. Most of these could be traced directly to effects induced by the relatively high power of the airplane (2100 hp, military rating). The desirability of adopting a dual-rotation propeller in order to improve the airplane characteristics was discussed at the time of the tests made with the single-rotation propeller. Hence, at the request of the Bureau of Aeronautics, Navy Department, the investigation with a four-blade dual-rotation propeller reported herein was conducted. To separate as completely as possible the effects due to a change in propellers, the model remained essentially unchanged. It is felt that these results, while specifically applicable only to the XSB2D-1 airplane, are indicative of what might be expected on any single-engine airplane.

The primary changes in the airplane characteristics anticipated from the use of the dual-rotation propeller were those due directly to the removal of the rotation from the slipstream. With the single-rotation propeller this rotation was such as to require 19° of right rudder deflection (85 percent of the available deflection) to hold the airplane at zero yaw in wave-off (i.e., a condition resulting from an unsuccessful landing attempt wherein full power is applied at minimum speed giving maximum values of thrust and torque). Alleviation of this rudder

deflection requirement is most desirable since the positive yaw attainable is unduly restricted. Surveys at the hinge line of the horizontal tail showed the asymmetric distribution of the downwash which normally results from the rotation of the slipstream of the single-rotation propeller. (At the wave-off torque coefficient helix angles as great as 11° were measured.) It was expected that the effective downwash angle at the tail would be altered but whether favorably or not could not be predicted.

A change in the location of the slipstream was also expected from the change to a dual-rotation propeller. The surveys taken with the single-rotation propeller operating showed that the greater percentage of the slipstream flowed over the right side of the tail. This resulted in the vertical surface passing out of the slipstream at small ($\cong 8^\circ$) angles of positive yaw and large ($\cong 16^\circ$) angles of negative yaw. At the point where the tail passed out of the higher dynamic pressure of the slipstream, the yawing moment contributed by the tail decreased and directional instability resulted. It was expected that, with the dual-rotation propeller, the slipstream would be symmetrically disposed about the tail at zero yaw. The angles at which directional instability began to develop would be the same in both positive and negative directions of yaw. Further, as the airplane was yawed, the slipstream deviated in the direction of flow of the surrounding air and reduced the dihedral effect. To what extent this would be altered by the dual-rotation propeller was unpredictable. The change in the slipstream location would also affect the effective dynamic pressure and downwash angle over the horizontal tail, but the magnitude and direction of the change could not be foreseen.

The test results presented in this report are for those conditions believed to show most clearly the differences in characteristics dependent on propeller type, and for each propeller similar test conditions were chosen.

MODEL

The model used for the tests was a 3/16-scale powered model of the Douglas XSB2D-1. It was a single-engine scout-bomber type with an inverted gull-type wing. The wing section from the root to the break in dihedral angle was a modified NACA 65,2-2518 section which tapered to a

modified NACA 65,2-2515 section at the tip. Douglas-type 25-percent-chord vaned flaps extended from the fuselage to the ailerons. Whenever the flaps were extended, the tricycle landing gear was also extended. The wing chord line had 2° of incidence with respect to the thrust line and had no geometric twist. With the exception of those tests made to determine dC_m/di_t all tests were made with the horizontal tail at 0° of incidence with respect to the thrust line. For all tests the cowl and oil-cooler flaps were open 6°.

Throughout the tests the model had transition fixed along the 17-percent-chord line on both the upper and lower surfaces and extending to a point 0.28 semispan from the plane of symmetry. The vertical fin had 0° offset with the dual-rotation propeller and -2° offset with the single-rotation propeller.

The propeller blades used were models of the Hamilton Standard design number 6457A-6. These have a high-speed (NACA 16 series) section and NACA cuffs.

Figure 1 is a three-view drawing of the model. Figures 2 and 3 show the model with the single-rotation and with the dual-rotation propellers, with the flaps retracted and with the flaps extended to 38°.

When received, the model was equipped only for single rotation. In order to accommodate the dual-rotation mechanism, a new cowl was made on which the leading edge was moved slightly aft from its location on the original cowl. A new spinner, slightly longer than the original, was required to cover the two hubs and the reversing mechanism. Figure 4 shows the relative locations of the single- and dual-rotation propeller disks, all with respect to the center of gravity of the airplane. It was necessary to increase the over-all propeller diameter from 28½ to 30½ inches on the dual-rotation propeller.

The single-rotation propeller was set at a blade angle of 21° and the dual-rotation propeller (both rear and front blades) was set at a blade angle of 21.6°. With the dual-rotation propeller installed, surveys were taken with a yawmeter immediately behind the rear propeller disk. For all values of V/nD and any radius less than 0.95R the twist in the slipstream was found to be zero.

TESTS AND RESULTS

Tests with each propeller were made at several values of thrust coefficient, and the test results were then cross-plotted to obtain the variation of the desired characteristics with lift coefficient for several constant power conditions. The variation of thrust coefficient with lift coefficient for the chosen power conditions (40 percent take-off power, 920 hp; normal rated power, 2100 hp; and 100 percent take-off power, 2300 hp) is shown in figure 5. The variation of lift coefficient with the angle of attack for each of the chosen power conditions and for the flaps undeflected and deflected to 38° is shown in figure 6. Figures 7 to 9 show, for similar conditions, the variation of the pitching-moment coefficient with the lift coefficient. The variation with angle of attack of the effective dynamic pressure at the horizontal tail as determined from the ratio of $(dC_m/di_t)_{\text{power on}}$ to the $(dC_m/di_t)_{\text{power off}}$ is shown in figure 10. The variation of the effective angle of attack of the horizontal tail as determined from the relation $\frac{C_{m_{tail}}}{(dC_m/di_t)}$ is shown in figure 11.

Yaw tests were made at several angles of attack, with the flaps retracted and with the flaps extended, at several values of thrust coefficient, and for several rudder deflections. Since the test results showed that the effects of the propeller type varied only in magnitude with the angle of attack and angle of flap deflection, only that condition showing the greatest effect is presented here. This was the approach condition with the model at 7.6° angle of attack in the wind tunnel, the landing gear extended and the flaps deflected to 38°. Figures 14 to 16 show the effect of power and of the propeller type on the variation of rolling-moment coefficient and yawing-moment coefficient with angle of yaw. These characteristics only are presented since they alone were affected by the change in propeller.

The test results are presented in standard NACA coefficient form and are referred to the stability axes. Model dimensions used are listed in the following table. It should be noted that for the dual-rotation propeller

the thrust coefficient T_c is based on the increased propeller-disk area. All coefficients have been corrected for tares and for wind-tunnel-wall effects.

b	span, feet	8.438
S	area, square feet	13.181
$\bar{c}$	mean aerodynamic chord, feet	1.627
D	propeller diameter, feet (single-rotation propeller)	2.375
	(dual-rotation propeller)	2.52

T_c effective thrust coefficient $= \frac{T_e}{\rho V^2 D^2}$

T_e measured thrust at 0° angle of attack, pounds

DISCUSSION

Longitudinal Stability

The power-on static longitudinal stability of the airplane has been shown to be a function of the following:

(1) The direct propeller forces, normal to and along the thrust line

(2) The effect of the slipstream on the pitching moment of the wing-fuselage combination

(3) The rate of change of effective downwash angle at the horizontal tail

(4) The rate of change of the effective dynamic pressure at the horizontal tail

For each of the chosen power conditions and for the flaps at 0° and 38° these effects have been separated, and for each power condition the magnitude of the effect with the dual-rotation propeller and with the single-rotation propeller is compared. Figures 7 to 9 show the build-up of the final power-on stability curves accomplished by adding to the power-off stability curves the

various power effects. The stability curve thus obtained is also compared with the experimentally determined curve. Figure 12 and 13 compare the magnitude of the various power effects for each propeller in terms of ΔC_m and shift of the neutral point.

The direct propeller forces increased with angle of attack and with power as predicted from theory. Their magnitude, however, was considerably greater than that predicted. From the data available it was impossible to ascertain the origin of this difference. The pitching-moment increments due to the direct propeller forces of the dual-rotation propeller are, at low values of lift, equal to, and at higher values of lift, as much as 20 percent greater than, those due to the single-rotation propeller. The direct propeller forces were responsible for about 50 percent of the destabilizing effects due to power when the flaps were undeflected and for about 30 percent of the instability when the flaps were deflected to 38°.

It has been assumed that the slipstream had no effect on the stability of the wing-fuselage combination when the flaps were undeflected. With the flaps deflected, their negative pitching moment was increased with increasing lift and the accompanying higher dynamic pressure in the slipstream. This stabilizing effect was sufficient to overcome about 30 percent of the total destabilizing effects due to power. This effect was slightly greater with the dual-rotation propeller, probably due to the removal of the slipstream rotation.

With the flaps undeflected the increased rate of change of downwash angle at the tail (fig. 11) accounted for about 50 percent of the destabilizing effects due to power. The effect is almost directly proportional to the power simulated. With full power the two propellers have an almost equal effect; at the lower power the dual-rotation propeller was slightly less destabilizing than the single-rotation propeller. At the higher angles of attack it can be seen that the horizontal tail surface was very nearly at zero angle of attack. When the flaps were extended to 38°, the change in the downwash angle at the tail due to power accounted for about 20 percent of the total destabilizing effects of power. The rate of change of downwash angle with the model angle of attack was not greatly increased with the increase in power (fig. 11), nor did a significant difference exist between that measured with the dual-rotation and with a single-rotation propeller. The most important effect of the change in

downwash was that it held the horizontal tail at large negative angles of attack.

The effect of the increased dynamic pressure was almost negligible when the flaps were undeflected (fig. 12). At low lift coefficients only a small increase in dynamic pressure was indicated, and at the higher lift coefficients, when the dynamic pressure was measurably increased, the tail was at almost zero angle of attack. With partial power, when the tail had positive lift, the effect was slightly stabilizing. With full power, when the tail had negative lift, the effect was slightly destabilizing. When the flaps were deflected to 38°, the increase in dynamic pressure became the most powerful destabilizing factor (figs. 8 and 13), because the tail was carrying negative lift. With full power and the dual-rotation propeller, this effect accounted for 50 percent of the total destabilizing effects of power. With the single-rotation propeller the effect was less because of a 20-percent lower effective dynamic pressure, despite a 1° greater negative effective angle of attack at the tail (fig. 11). It accounted for only about 35 percent of the total destabilizing effects of power. At the lower power similar results existed but of a lesser magnitude.

With the center-of-gravity location assumed (0.25 M.A.C.) the tail would be required to carry but little lift to trim. If a sufficient rearward movement of the center of gravity occurred, the tail would be required to carry an appreciable upload at all times. In this case the increased dynamic pressure would exert a powerful stabilizing effect. To illustrate the magnitude of this effect, the effects of power on the stability have been separated for a case of the elevator deflected to 5° (fig. 9). Here, throughout the angle-of-attack range, the tail was carrying positive lift. The increased dynamic pressure was able to overcome about 20 percent of the destabilizing effects of power in this condition.

No significant change in either elevator effectiveness or elevator hinge moment was measured after installation of the dual-rotation propeller other than the increase to be expected from the higher dynamic pressure experienced at the horizontal tail.

Considering the effects as a whole, it can be seen that with the flaps undeflected, power was slightly more

destabilizing with a dual-rotation propeller because of larger propeller forces. With the flaps deflected to 38°, greater instability was shown with the dual-rotation propeller, partly due to greater propeller forces, but, to a greater extent, due to a higher effective dynamic pressure acting on a horizontal surface which was carrying negative lift.

Directional Characteristics

The effects of power on the directional characteristics of an airplane are a function of the following:

(1) The propeller forces normal to the thrust line

(2) The effect of the slipstream on the directional characteristics of the wing-fuselage combination

(3) The change in the angle of sidewash over the vertical surface induced by rotation in the slipstream

(4) The increase in dynamic pressure over the vertical surface

(5) The disposition of the slipstream with respect to the vertical surface

As noted earlier, the simulated wave-off condition was chosen for presentation here since at this condition the highest thrust and torque coefficients occur and the above effects were found to be almost wholly a function of these two factors and essentially independent of angle of attack and flap deflection. While, unlike the longitudinal characteristics, it is impossible to separate quantitatively the effects of the various factors, it is possible from the results to infer to a considerable extent their individual effects. Figure 14 presents the effects of full power (wave-off condition) and of tail surfaces on the yawing-moment characteristics of the model with a dual-rotation and with a single-rotationn propeller. Figure 15 shows the effect of full power (wave-off condition) and of the dual- and single-rotation propeller on the rudder control.

From the data at hand it was impossible to separate the direct propeller forces and the slipstream effect on

and the fuselage. The summation of their effects may be seen in the rotation and the displacement of the curves of the variation of yawing-moment coefficient with angle of yaw. Whereas full power rotates the curves an almost identical amount ($\Delta dC_n/d\psi = 0.0013$) with both types of propeller, the single-rotation propeller caused a shift in the yawing-moment coefficient at zero yaw (from 0 to -0.017) which did not occur with the dual-rotation propeller (fig. 14). The first effect probably is due to propeller forces normal to the thrust line plus the effect of the slipstream on the wing and the fuselage. The second effect is due to rotation of the slipstream in one case, since helix angles as great as 11° were measured at the corresponding thrust coefficient, and to lack of rotation in the other.

With the tail installed, both propellers increased the directional stability (from $dC_n/d\psi = -0.0017$ to $dC_n/d\psi = -0.0035$), when operated at a thrust coefficient corresponding to full power. This would indicate slipstreams of about equal intensity from the two propellers. It should be noted that this increase in directional stability is not a true measure of the effectiveness of the vertical surface. It has been shown that, with full power and with the tail removed, both propellers increased the directional instability. The vertical surface, therefore, overcame this additional instability as well as increased the power-off directional stability. To do this, the vertical surface supplied at least twice as great a yawing-moment coefficient with propellers operating as it did with the propellers removed. As was found with the tail removed, the single-rotation propeller induced a yawing moment at zero yaw ($C_n = -0.038$) while the dual-rotation propeller did not - the yawing moment at zero yaw remaining essentially zero. This is probably the most significant change in the airplane characteristics that resulted from installation of the dual-rotation propeller. It is evident from figure 15 that, with the dual-rotation propeller, adequate directional control is maintained at all powers and in positive or negative yaw. In contrast, with the single-rotation propeller the negative yaw available is inordinately high ($<-30°$) and the positive yaw is undesirably low (5°). A rudder deflection of $-19°$ is required to hold zero yaw.

Previous analyses have shown that the location of the slipstream at the tail has a powerful effect on the

directional characteristics of an airplane. The effectiveness of the vertical surface dropped as it passed out of the slipstream. With appreciable power directional instability resulted, since the yawing moment provided by the vertical surface was insufficient to overcome the unstable yawing moments due to propeller forces and to the wing–fuselage combination (fig. 14). If the airplane reaches trim before this occurs, it becomes a matter of small consequence. If, however, the vertical surface passes out of the slipstream before the airplane reaches trim, high angles of yaw will be encountered with full rudder deflection. With the single–rotation propeller the vertical surface passed out of the slipstream at about -23° yaw and 15° yaw, indicating an asymmetry of slipstream location (fig. 14). With full (25°) positive rudder deflection, a condition of zero yawing moment was not reached before the vertical surface moved out of the slipstream. Yaw angles of greater than 30° were required to reach this trimmed condition. The slipstream from the dual–rotation propeller was symmetrically located, and the vertical surface passed out of it at $\pm 15^\circ$ yaw. Because no yawing moment was required to hold zero yaw, the model could be trimmed in yaw at $\pm 17^\circ$ with full–rudder deflection before the vertical surface lost its effectiveness.

Lateral Stability

The major effect of the dual–rotation propeller was to make the lateral stability of the model symmetrical about zero yaw. No significant improvement in the stability over that experienced with the single–rotation propeller was observed.

With both types of propeller, power had a destabilizing effect upon the lateral stability of the model. The destabilizing effect increased with lift coefficient and with power. The dual–rotation propeller gave evidence of having the greater effect, particularly at negative angles of yaw. The origin of this destabilizing moment has been shown to lie in the diversion of the slipstream over the trailing wing when the model was yawed. The increased lift engendered by the slipstream was thus placed so as to produce a destablizing force the moment arm of which increased as the model was yawed. An investigation was made with both the single– and dual–rotation propeller installed to determine the location of the slipstream on the

wing at various angles of yaw. The results (fig. 17) show that the slipstream moved across the wing in almost exactly the same manner with either propeller. Since it has been shown that this effect produces the major change in lateral stability, it might be expected that any change due directly to propeller type would be of secondary importance. Experiment bore out this conclusion in that the measurable differences between the results from the two propellers were minor and could not be traced to one source but appeared to be the summation of a number of secondary effects.

With neither propeller did the reaction torque appear in the rolling-moment results. Zero slipstream twist, the necessary and sufficient condition for no reaction torque, has already been shown to have existed with the dual-rotation propeller. Predictions based on theory (reference 1) and experiment showed that with the single-rotation propeller the reaction torque was almost wholly compensated for by the straightening of the propeller slipstream by the wing.

The wave-off condition has been chosen for a quantitative discussion because it shows most strongly the effects of power on lateral stability. Figure 16 shows these results for the single-rotation propeller. With the tail off, the lateral stability ($dC_l/d\psi$) was changed from about 0.003 (near $\psi = 0$) to 0.001 with 40 percent take-off power and to −0.0005 with 100 percent take-off power. For the power-on conditions the stability over a narrow range of yaw was considerably improved by the addition of the tail. From a value of 0.003, power off, the stability changed only to 0.0015 with 40 percent take-off power and to 0.0005 with 100 percent take-off power. This stabilizing effect of the tail was found to extend only slightly into the range of positive yaw (10° or less), but the effect extended at least 5° farther into the range of negative yaw. At high values of positive or negative yaw the lateral stability approached that of the tail-off condition. It will be recalled from the directional-stability results that the slipstream was found to be displaced so that the tail was affected by it to higher values of negative than of positive yaw. It would appear from this that the tail will exert a stabilizing effect greater than that expected from its dihedral (7°) and span (20 in.) when it is in the slipstream.

Figure 16 (concluded) shows the effects of power and of the tail surfaces when the dual-rotation propeller was installed. With the tail off the lateral stability was changed from about 0.0028, power off, to 0.0007 with 40-percent take-off power and -0.0008 with 100 percent take-off power. As with the single-rotation propeller, the addition of the tail increased the stability over a limited yaw range, which was, however, symmetrically placed with respect to zero yaw. From a value of 0.0028, power off, the stability decreased only to 0.0015 with 40 percent take-off power and 0.0005 with 100 percent take-off power. The yaw range over which the tail had an appreciably stabilizing effect was about $\pm 6^{\circ}$. This again corresponds very closely to the yaw range in which the vertical surface remained in the slipstream and serves to verify the conjecture that the slipstream makes the tail a significant stabilizing factor.

CONCLUSIONS

The following conclusions can be drawn as to the comparable effects of the single- and dual-rotation propellers:

1. In pitch the dual-rotation propeller will be more destabilizing because of its greater direct propeller forces and because of a greater concentration of the slipstream at the tail with the attendant destabilizing effects.

2. The dual-rotation propeller will cause no change in $dC_m/d\delta_e$ or $dC_{h_e}/d\delta_e$ from that existent with the single-rotation propeller other than would be expected from the slight increase in q/q_o.

3. In general, the same change in characteristics in yaw with power may be expected with both dual- and single-rotation propellers. Two important differences, however, will exist. Where appreciable asymmetry exists between force-test results at positive and negative angles of yaw with the single-rotation propeller, almost complete symmetry will exist with the dual-rotation-propeller. Where the application of power with the single-rotation propeller will translate as well as rotate the curves of propeller-off results, the application of power

with the dual-rotation propeller will produce rotation only. This will result in the elimination of the rolling moment, yawing moment, and side force which exist at zero yaw with the single-rotation propeller.

4. No significant change in $dC_n/d\psi$ or $dC_n/d\delta_r$ will be occasioned by a dual-rotation propeller.

5. No difference of any consequence will be found between the lateral stability existent with the dual- or single-rotation propeller.

Ames Aeronautical Laboratory,
National Advisory Committee for Aeronautics,
Moffett Field, Calif.

REFERENCE

1. Ower E., Warden, R., and Pankhurst, R. C.: Interim Note on Wing-Nacelle-Airscrew Interference. British A.R.C. 4572 (A.P.234) (Ae.1668), June 6, 1940.

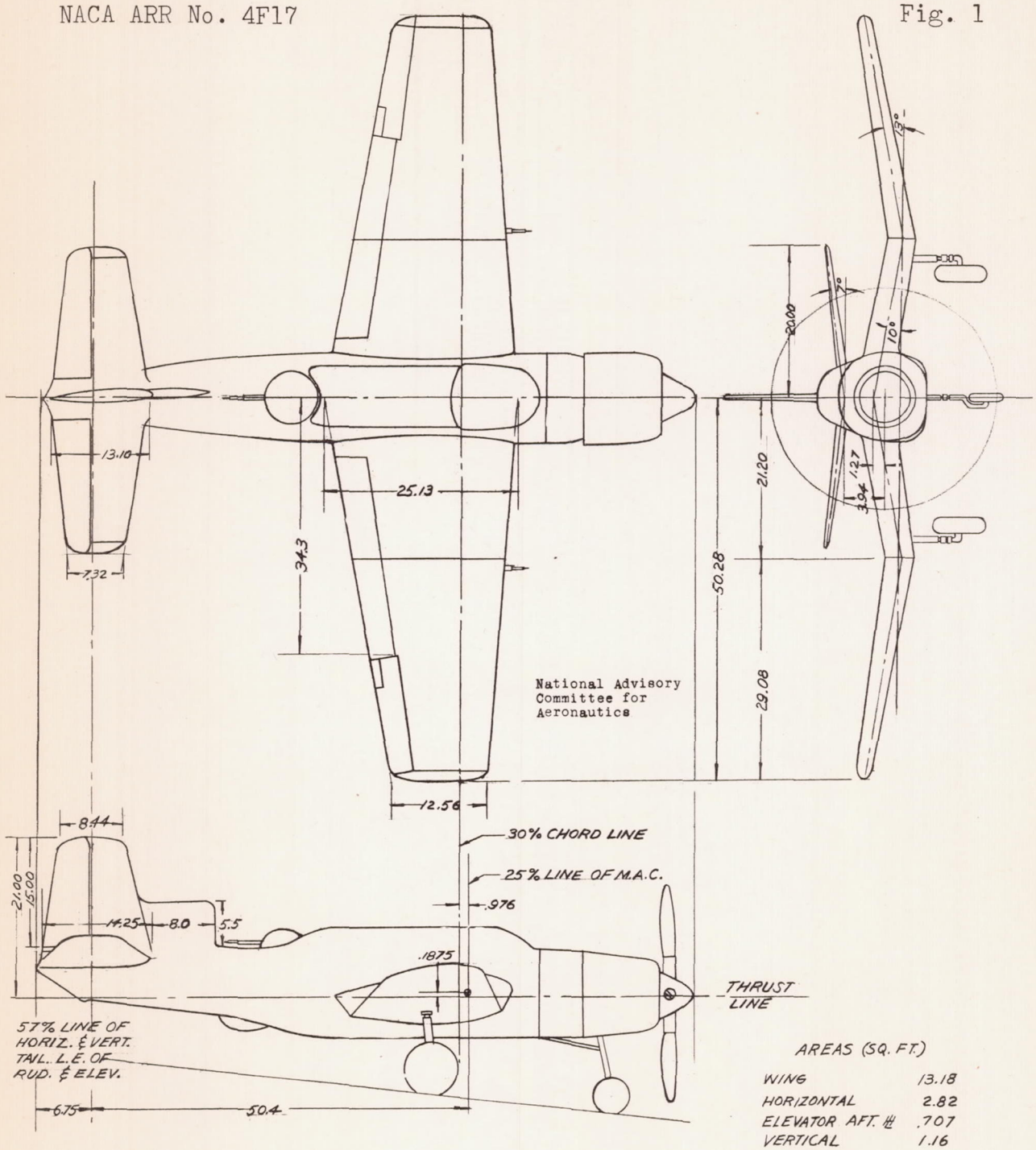

AREAS (SQ. FT.)

WING	13.18
HORIZONTAL	2.82
ELEVATOR AFT. ½	.707
VERTICAL	1.16
DORSAL	.31
RUDDER AFT. ½	.37

ALL DIMENSIONS ARE IN INCHES.

FIGURE 1.- THREE-VIEW DRAWING OF THE 3/16-SCALE MODEL OF THE DOUGLAS AIRPLANE XSB2D-1 WITH A SINGLE-ROTATION PROPELLER.

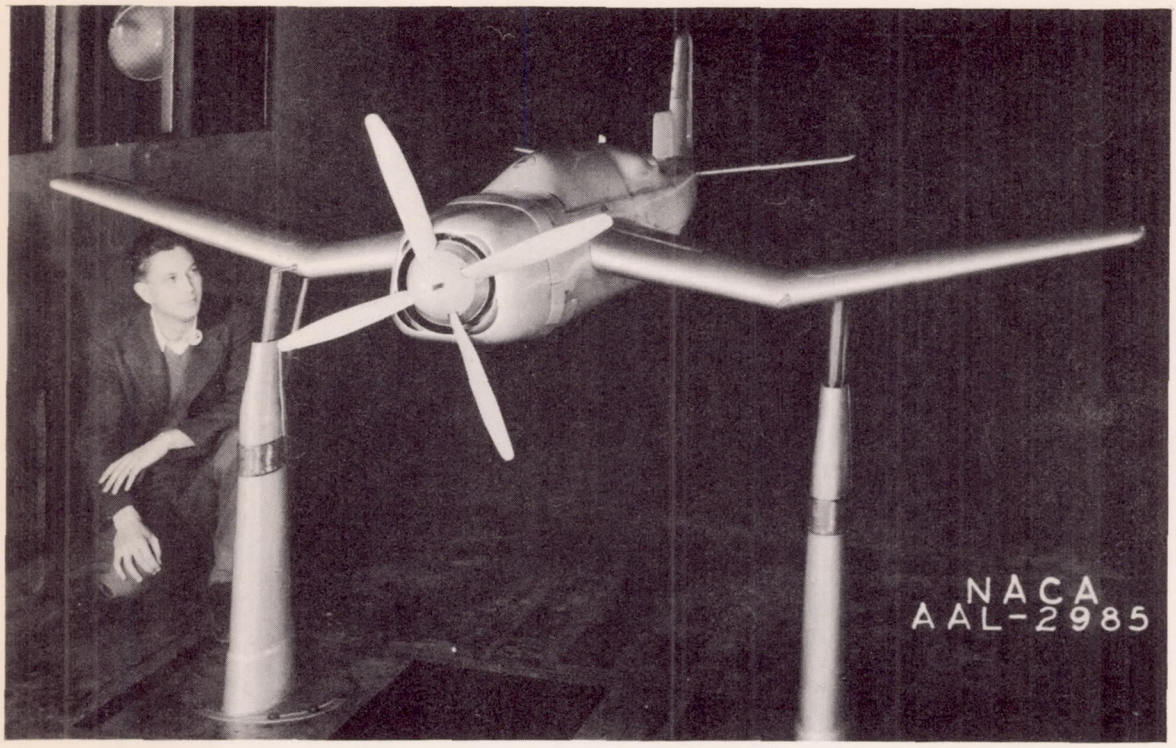

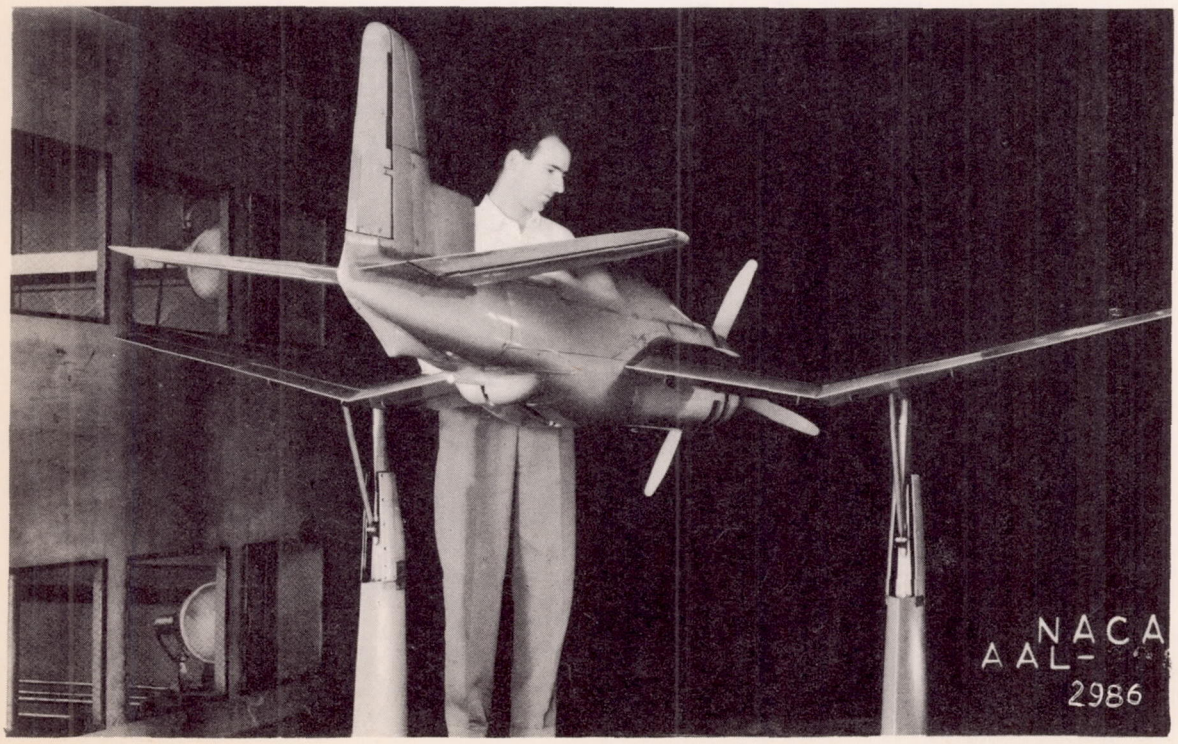

Figure 2.- A 3/16-scale model of the Douglas XSB2D-1 with flaps retracted and a single-rotation propeller.

A-43

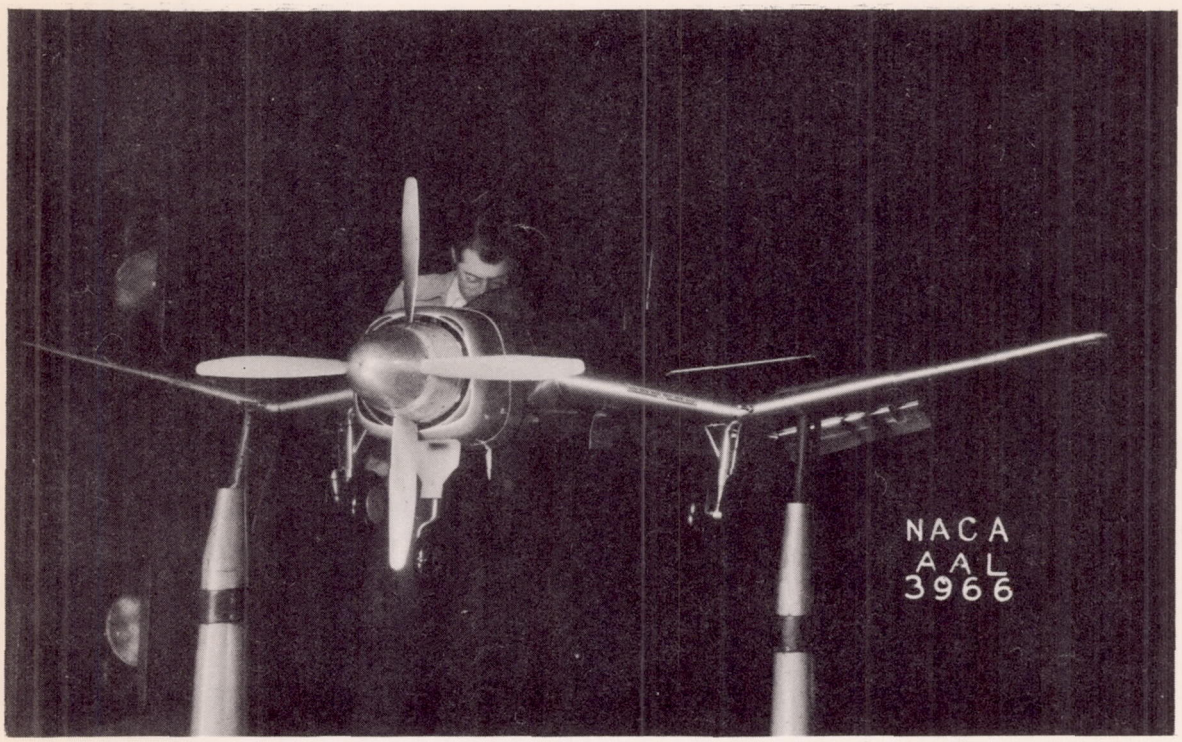

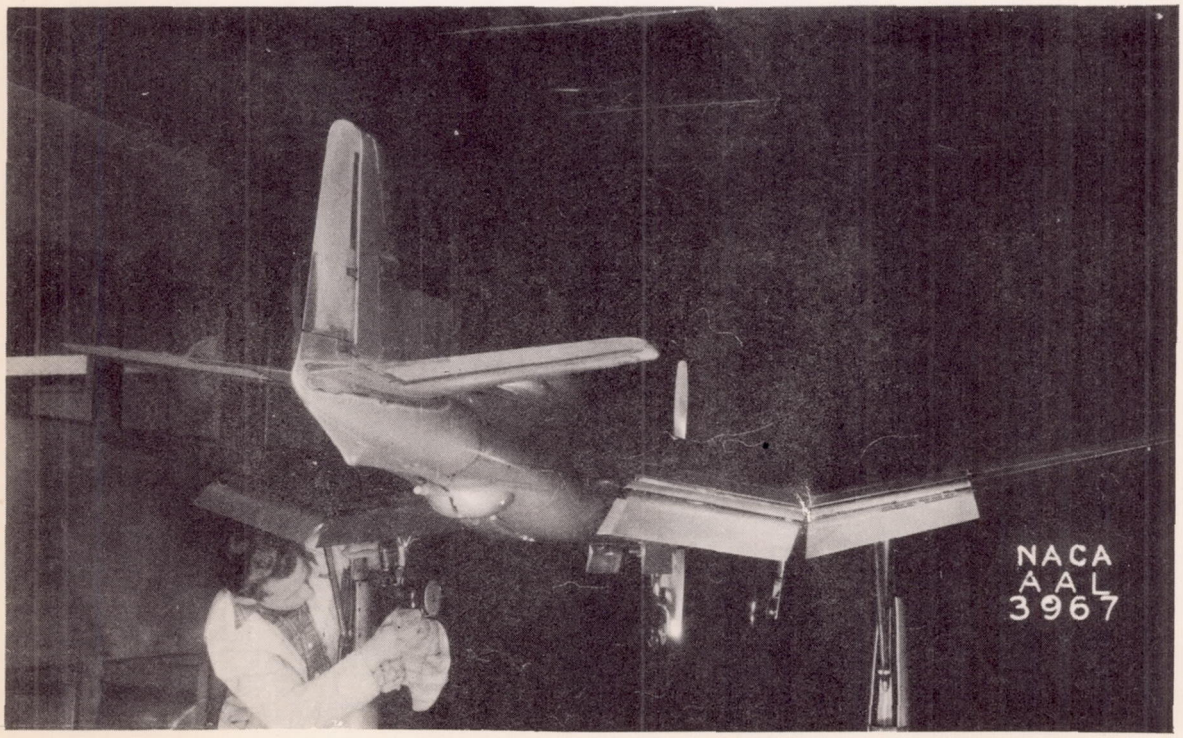

Figure 3.- A 3/16-scale model of the Douglas XSB2D-1 with flaps extended to 38° and a dual-rotation propeller.

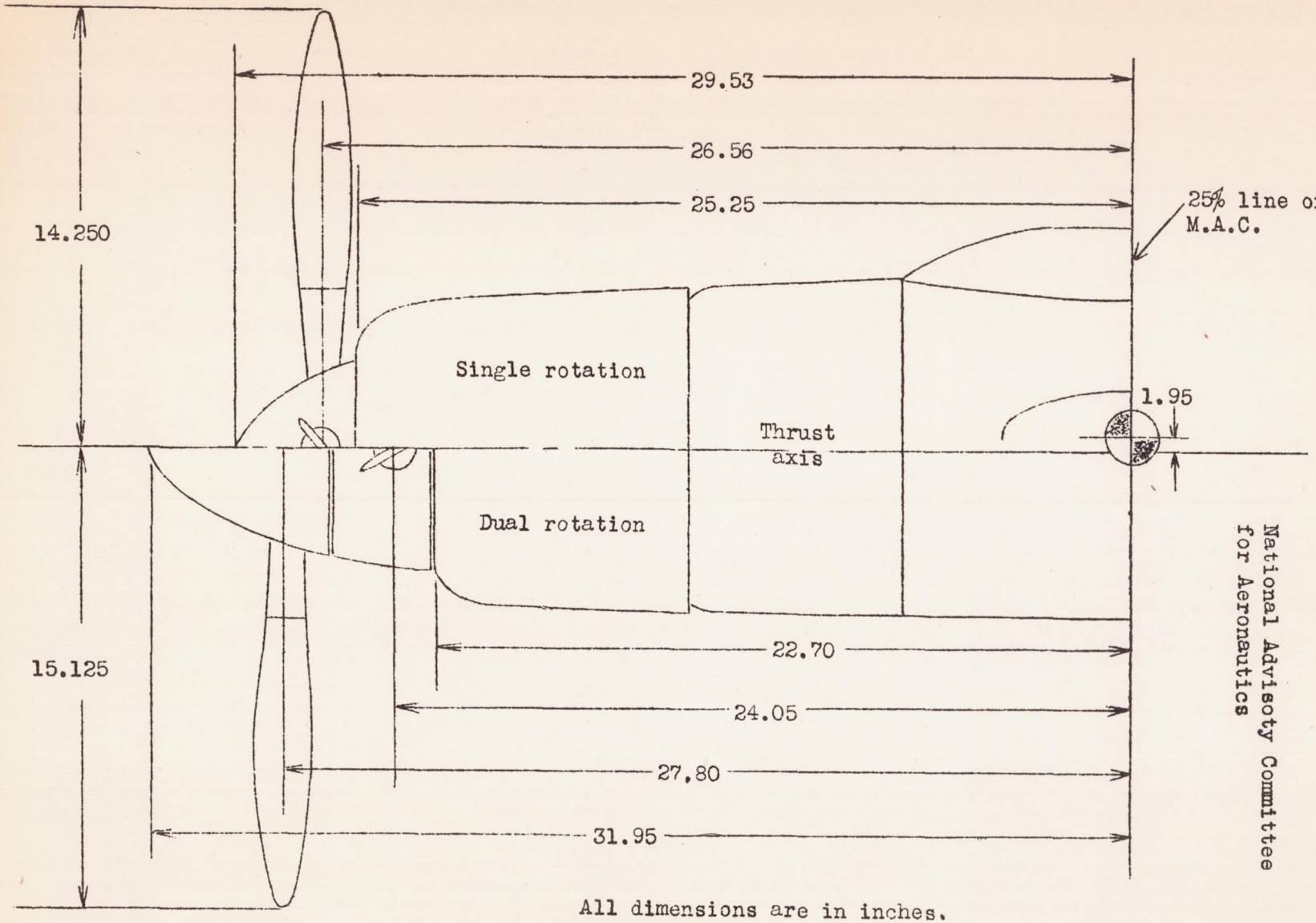

All dimensions are in inches.

Figure 4.- Locations of propeller, spinner, and cowl for single and for dual rotation. 3/16- scale model of the XSB2D-1 airplane.

NACA ARR No. 4F17

National Advisory Committee for Aeronautics

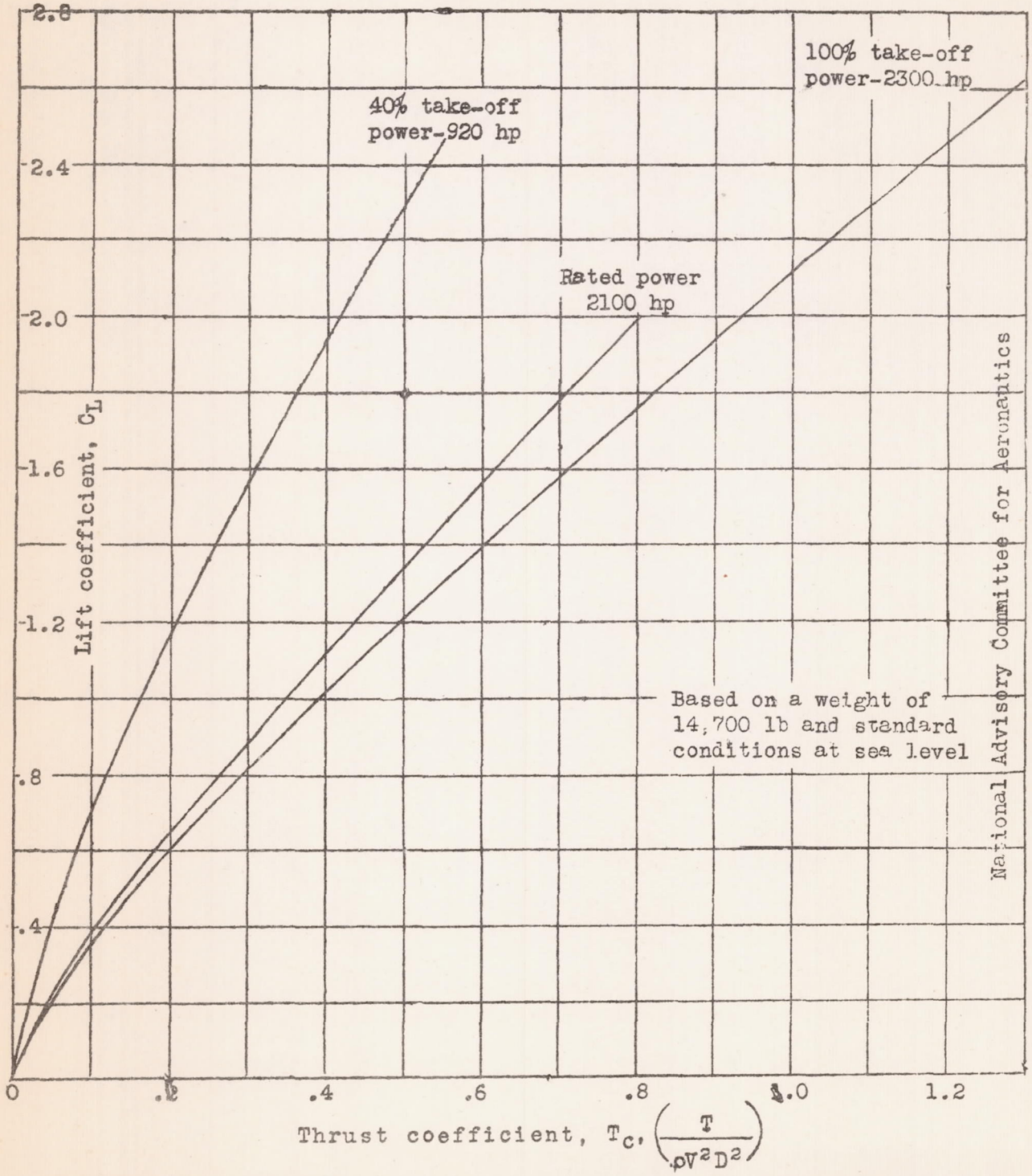

Figure 5.- The variation of thrust coefficient with lift coefficient for the XSB2D-1 airplane.

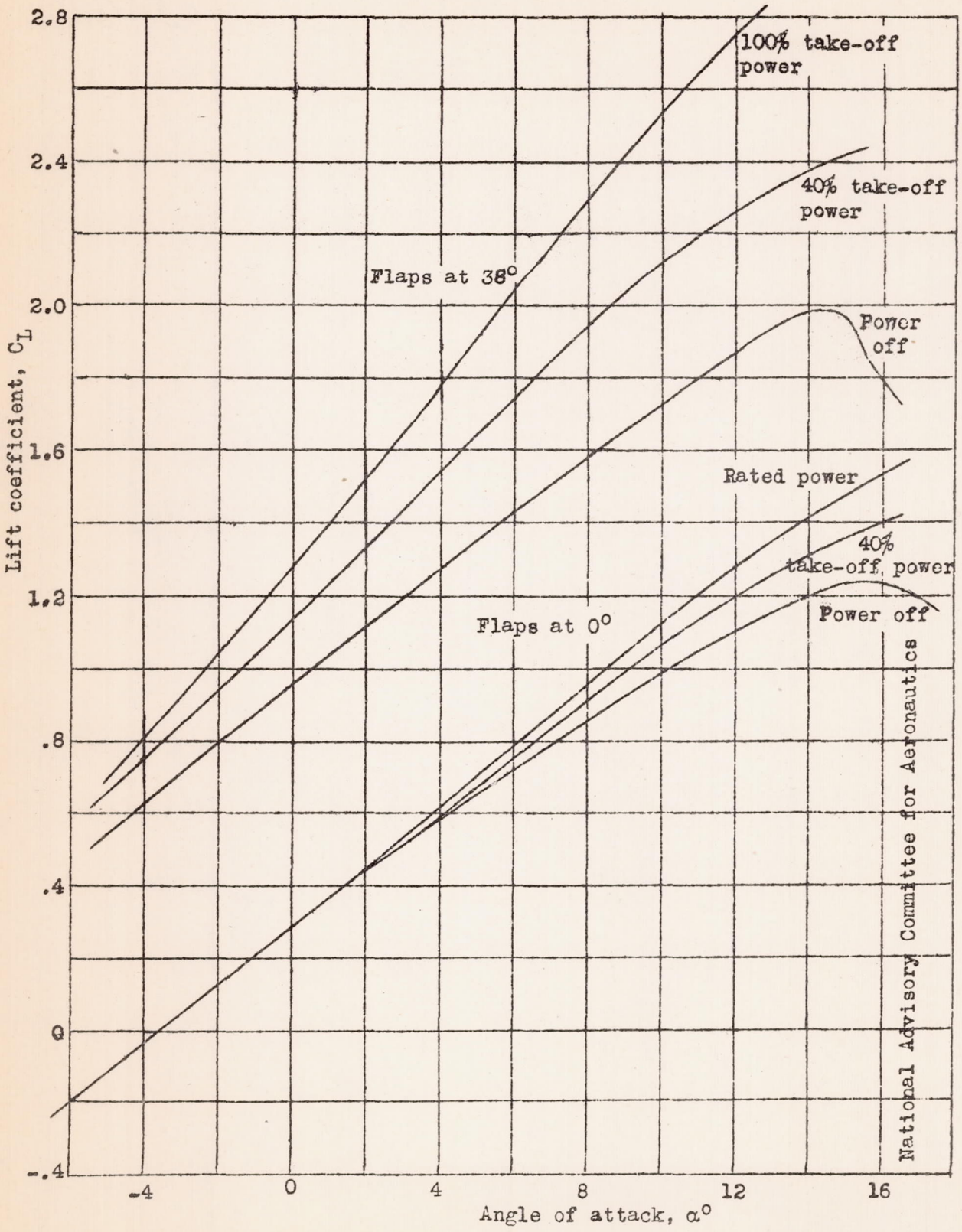

Figure 6.- The variation of lift coefficient with angle of attack for several powers and two flap positions, 3/16-scale model of the XSB2D-1.

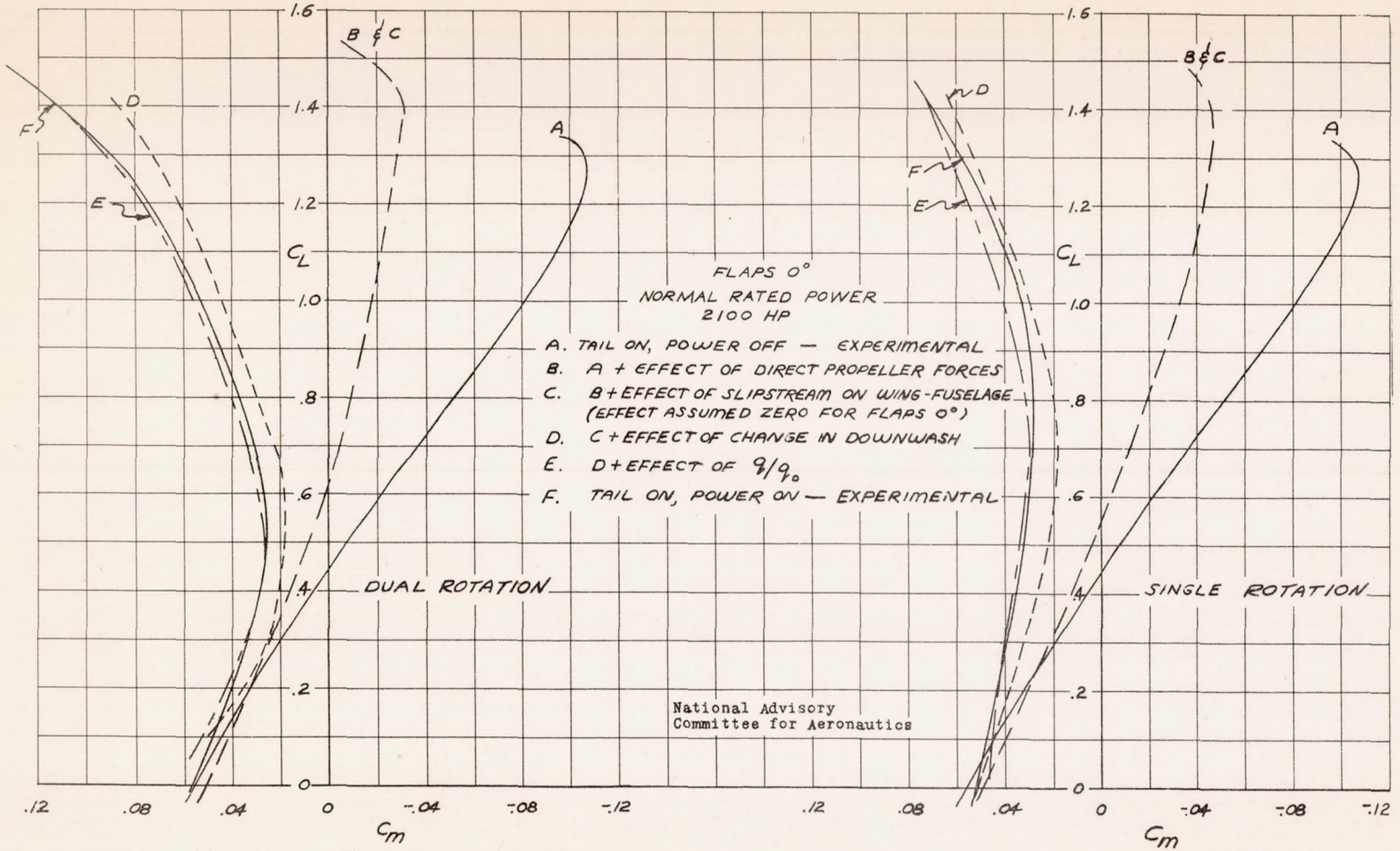

FIGURE 7a.- VARIOUS EFFECTS OF POWER ON LONGITUDINAL STABILITY OF THE XSB2D-1 MODEL. FLAPS UNDEFLECTED, 2100 HP.

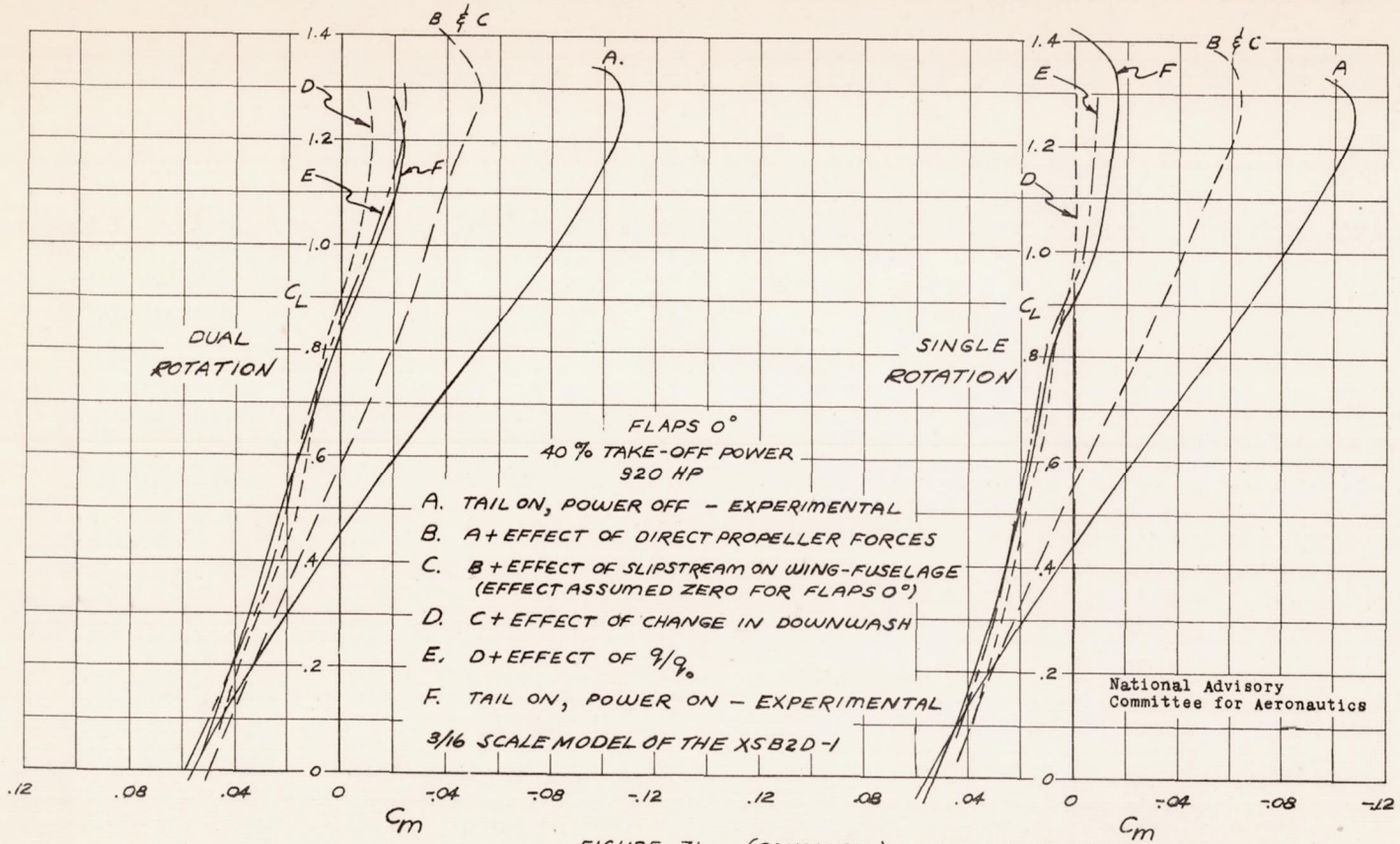

FIGURE 7b.- (CONCLUDED) FLAPS UNDEFLECTED, 920 HP.

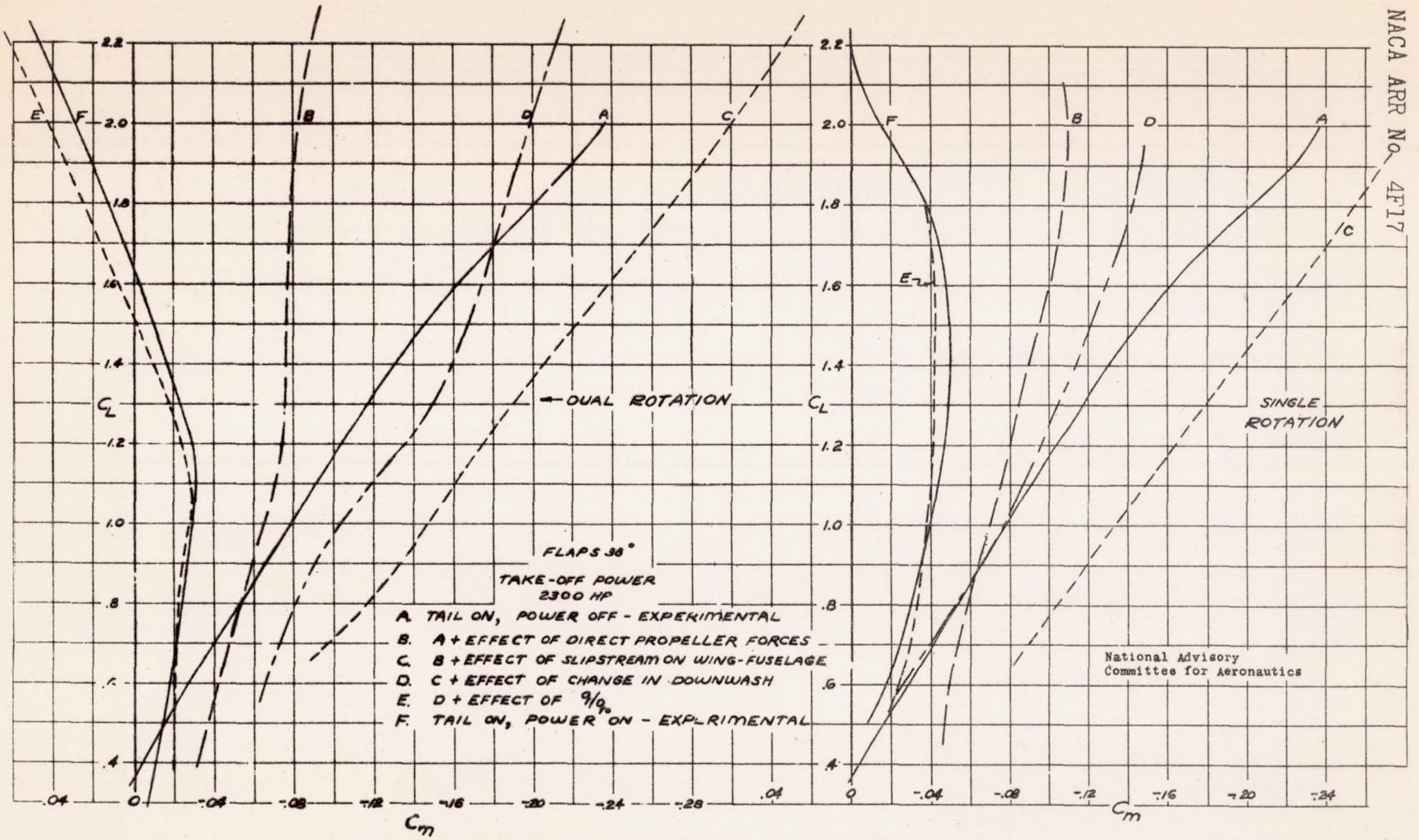

FIGURE 8a.- VARIOUS EFFECTS OF POWER ON LONGITUDINAL STABILITY OF THE XSB2D-1 MODEL WITH FLAPS DEFLECTED TO 38°, 2300 HP.

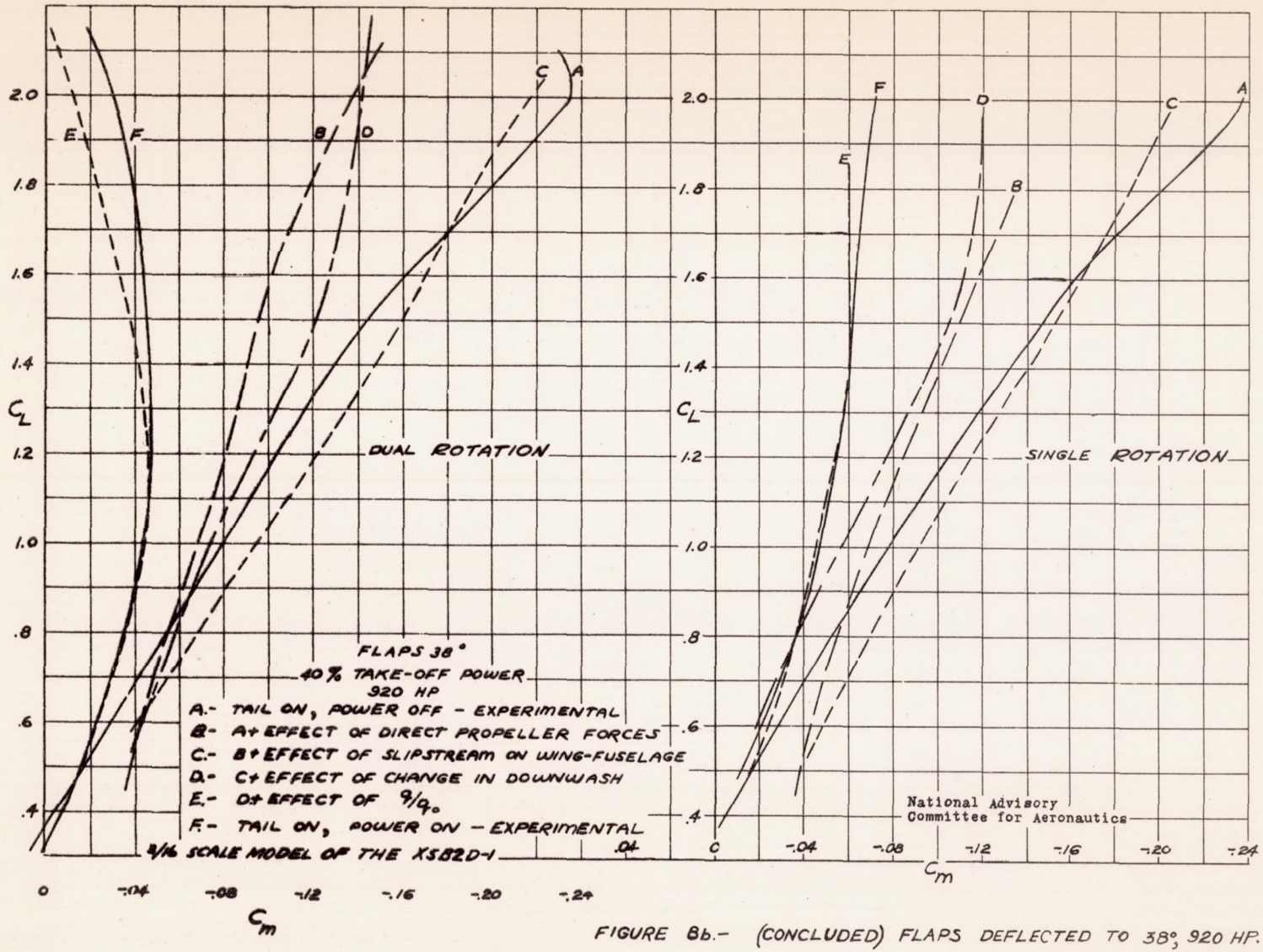

FIGURE 8b.- (CONCLUDED) FLAPS DEFLECTED TO 38°, 920 HP.

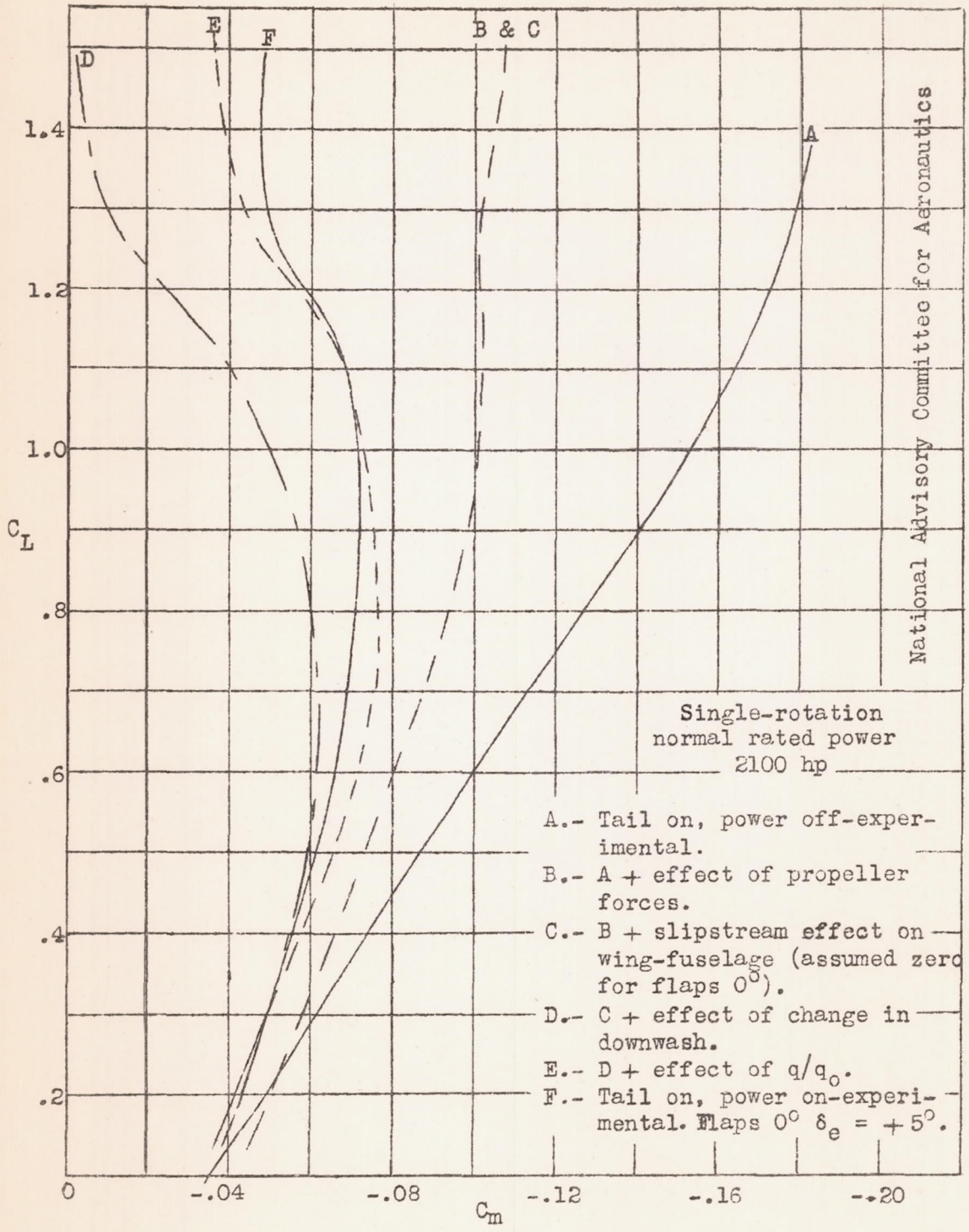

Figure 9.- Various effects of power on longitudinal stability of the XSB2D-1 model with flaps undeflected and with elevators deflected to +5°.

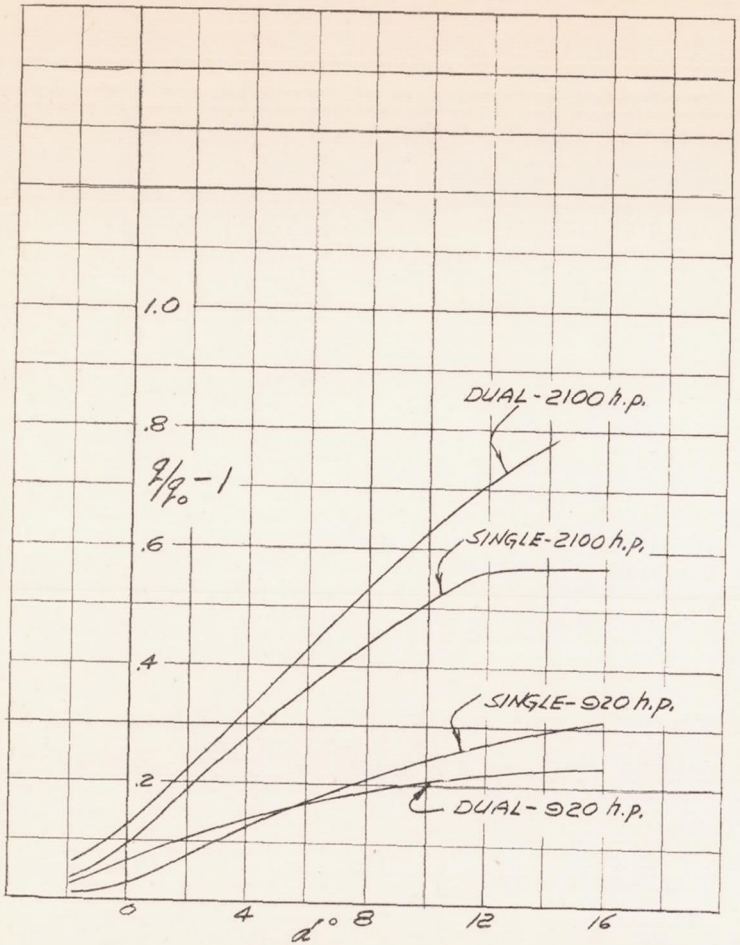

FLAPS UNDEFLECTED

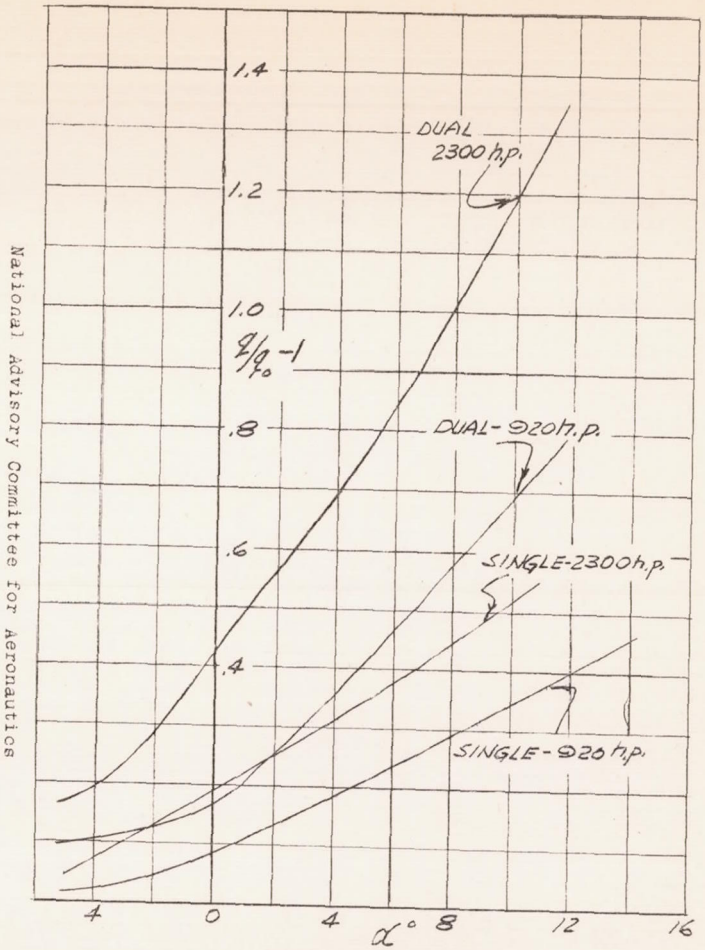

FLAPS DEFLECTED TO 38°

FIGURE 10. VARIATION OF THE RATIO OF EFFECTIVE DYNAMIC PRESSURE AT THE HORIZONTAL TAIL, POWER ON, TO THE EFFECTIVE DYNAMIC PRESSURE AT THE HORIZONTAL TAIL, POWER OFF, WITH ANGLE OF ATTACK OF THE MODEL, SHOWING THE EFFECT OF A DUAL- AND A SINGLE-ROTATION PROPELLER, FULL AND PARTIAL POWER, AND TWO FLAP POSITIONS, 3/16 SCALE MODEL OF THE XSB2D-1

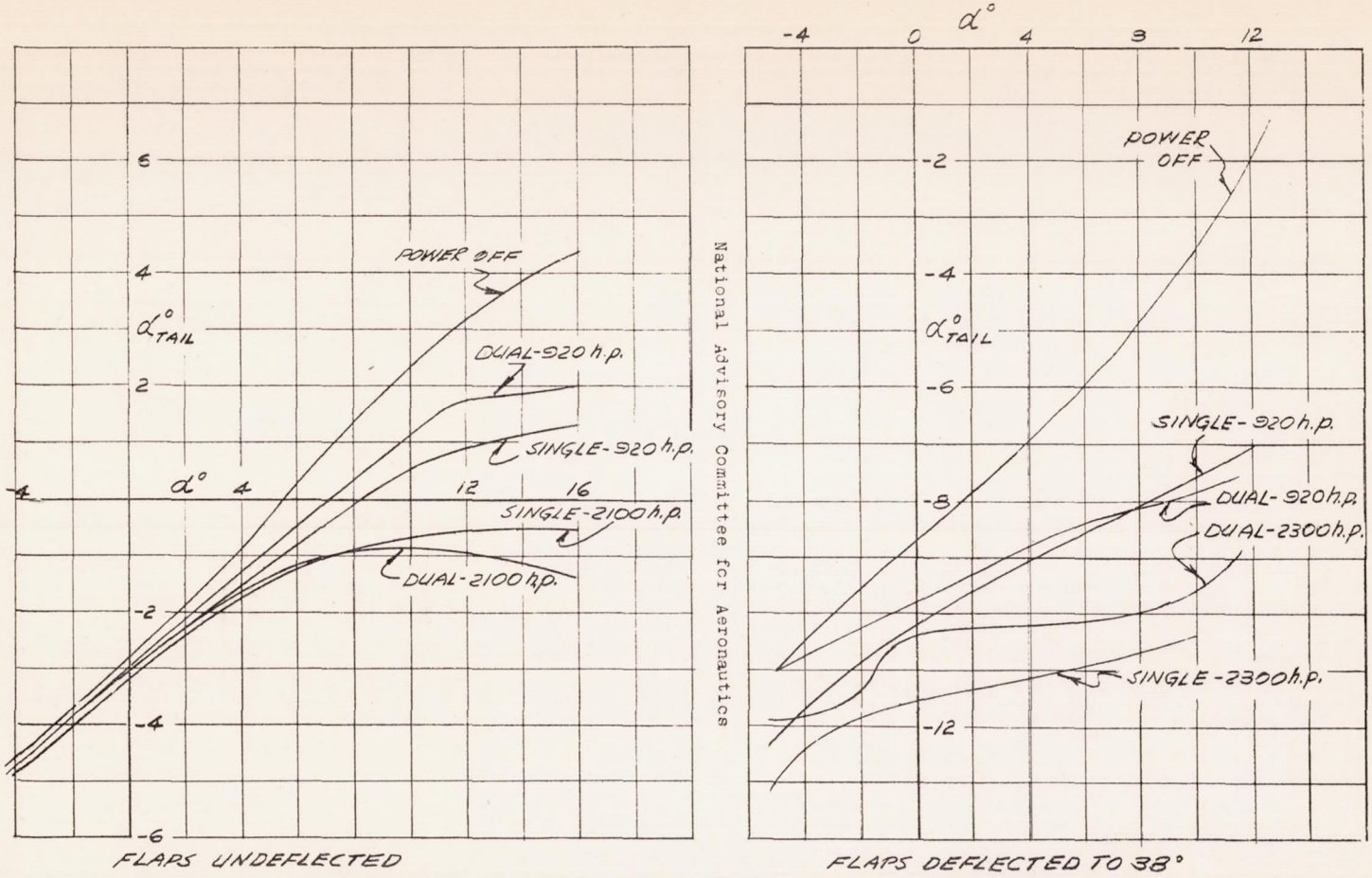

FIGURE 11. VARIATION OF THE EFFECTIVE ANGLE OF ATTACK OF THE HORIZONTAL TAIL WITH THE CORRECTED ANGLE OF ATTACK OF THE MODEL, SHOWING THE EFFECT OF A DUAL- AND SINGLE-ROTATION PROPELLER, FULL AND PARTIAL POWER AND TWO FLAP POSITIONS. 3/16 SCALE MODEL OF THE XSB2D-1.

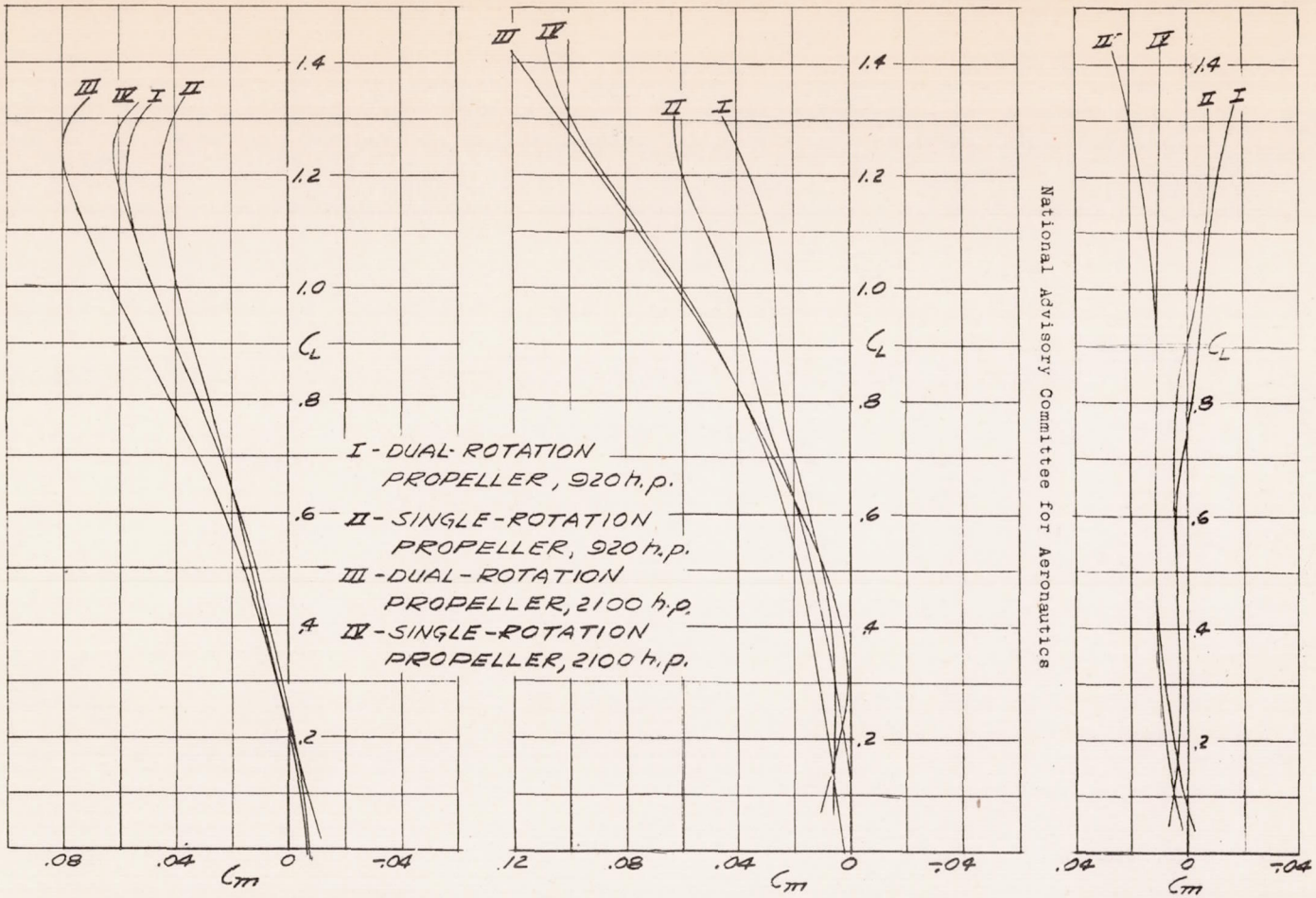

PITCHING MOMENT INCREMENT DUE TO DIRECT PROPELLER FORCES.

PITCHING MOMENT INCREMENT DUE TO INCREASED DOWNWASH ANGLE.

PITCHING MOMENT INCREMENT DUE TO INCREASED DYNAMIC PRESSURE

FIGURE 12 COMPARISON OF THE PITCHING MOMENT INCREMENTS, DUE TO POWER, OF A DUAL-ROTATION AND A SINGLE-ROTATION PROPELLER. FLAPS UNDEFLECTED AND @20 h.p. AND 2100 h.p. SIMULATED. 3/16 SCALE MODEL OF THE XSB2D-1.

(a)

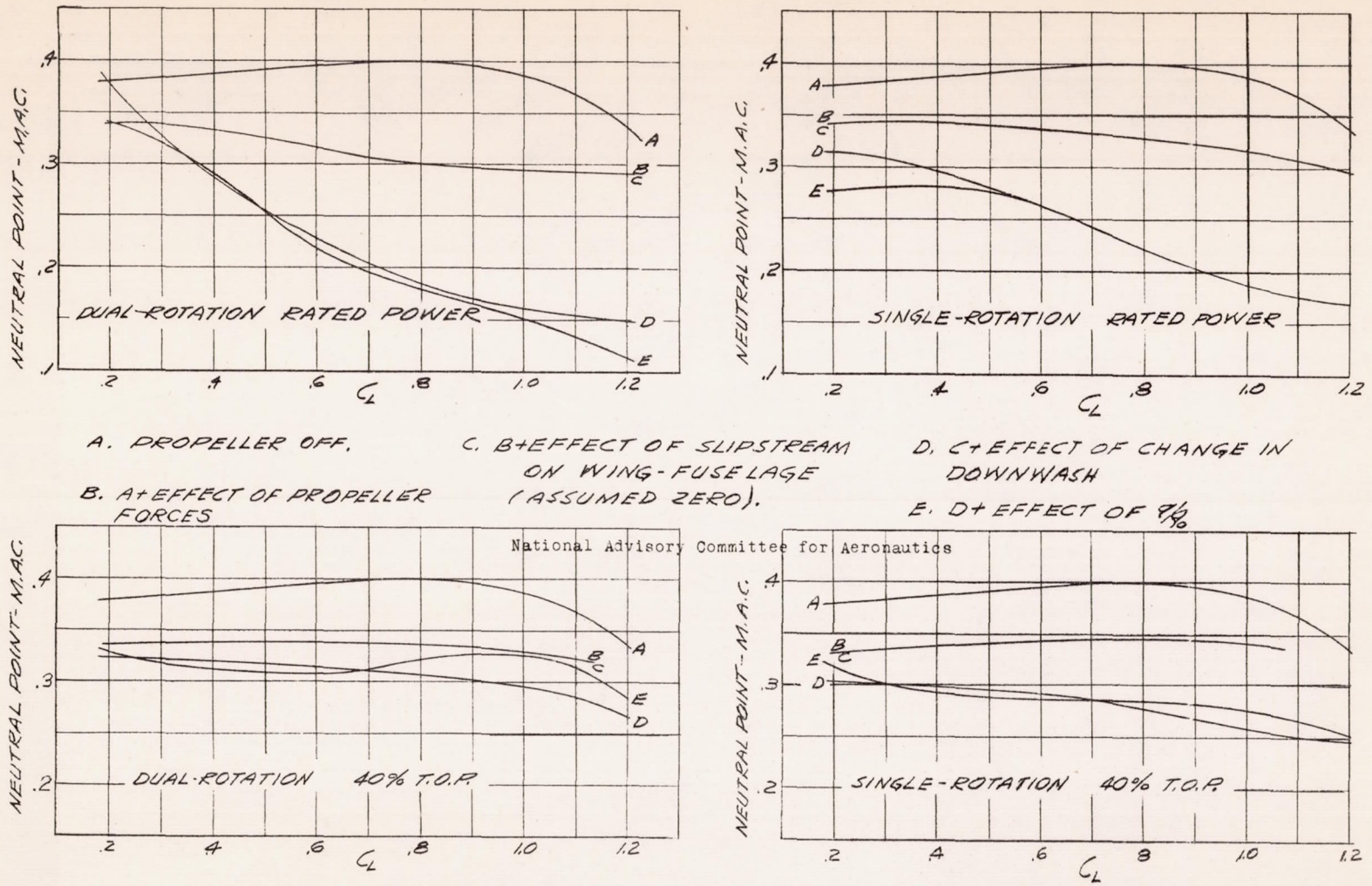

FIGURE 12 (CONCLUDED). SHIFT IN THE NEUTRAL POINT OF THE XSB2D-1 CAUSED BY THE VARIOUS EFFECTS OF POWER, FLAPS UNDEFLECTED.

(b)

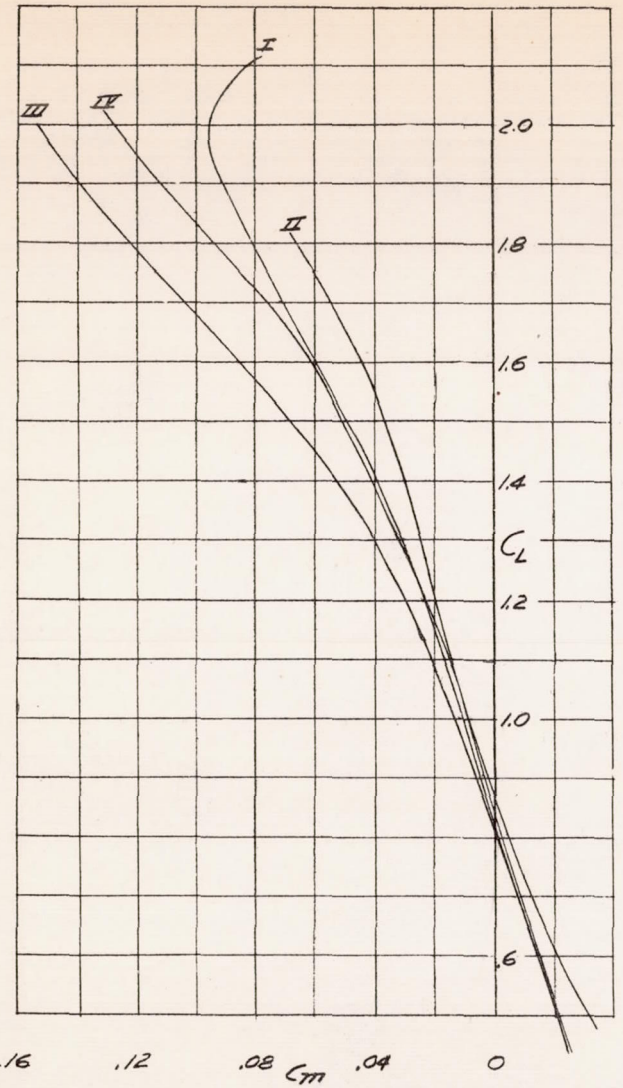

a.- PITCHING MOMENT INCREMENT DUE TO DIRECT PROPELLER FORCES.

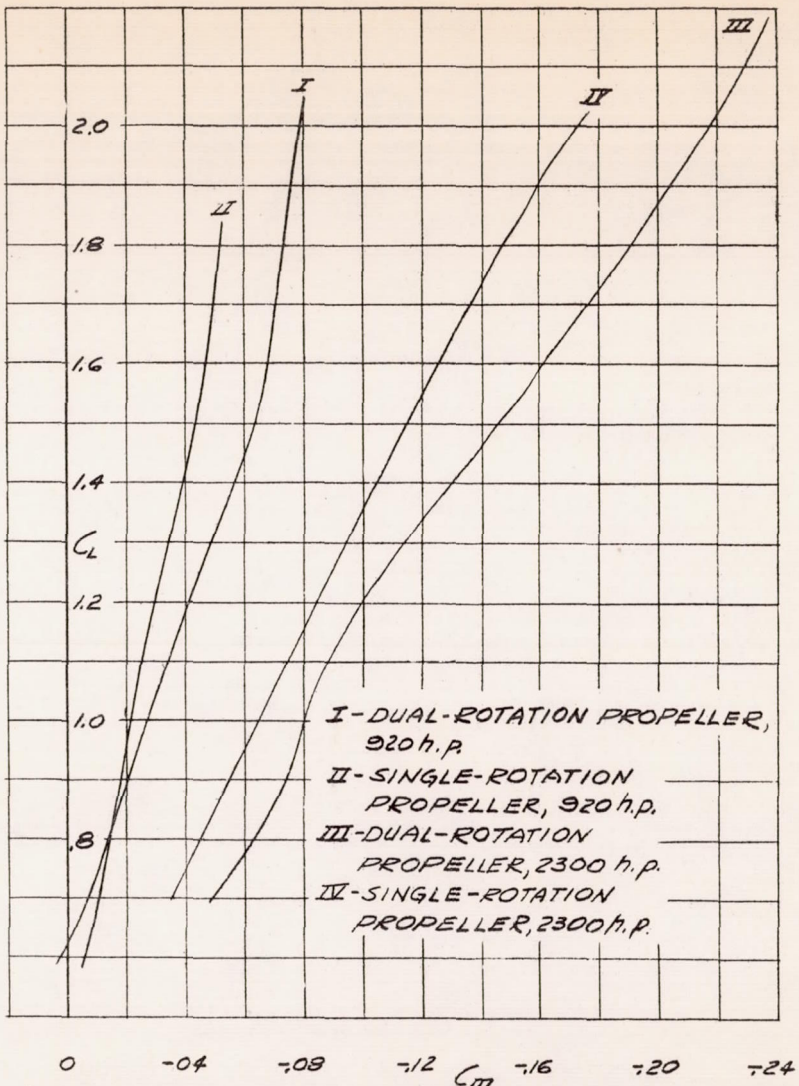

b.- PITCHING MOMENT INCREMENT DUE TO THE EFFECT OF SLIPSTREAM ON THE WING-FUSELAGE COMBINATION.

FIGURE 13.- COMPARISON OF THE PITCHING-MOMENT INCREMENTS, DUE TO POWER, OF A DUAL-ROTATION AND A SINGLE-ROTATION PROPELLER. FLAPS DEFLECTED TO 38° AND 920 h.p. AND 2300 h.p. SIMULATED. 3/16-SCALE MODEL OF THE X5820-1.

(a)

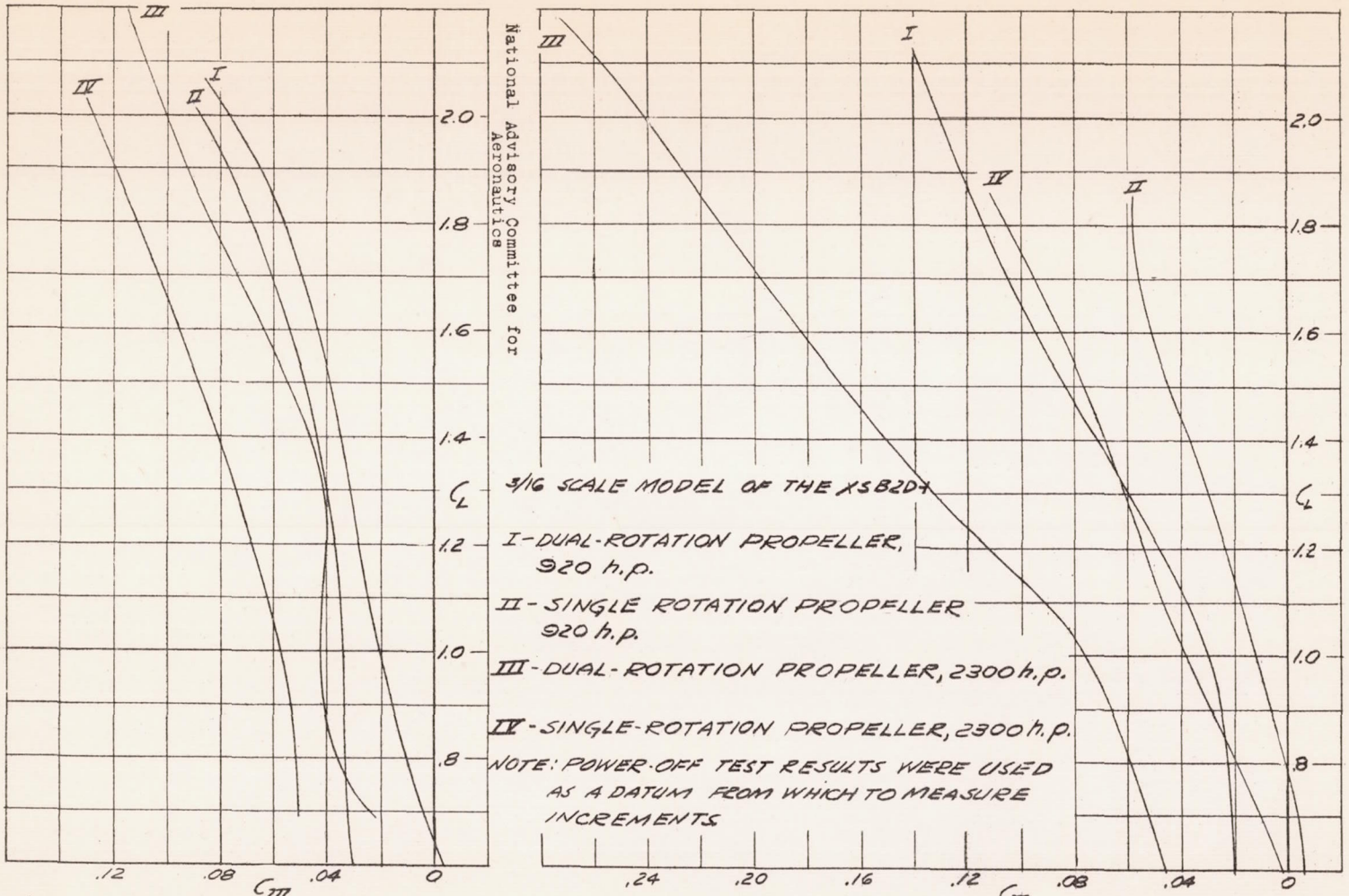

(a). PITCHING MOMENT INCREMENT DUE TO INCREASED DOWNWASH ANGLE.

(b). PITCHING MOMENT INCREMENT DUE TO INCREASED DYNAMIC PRESSURE.

FIGURE 13b.-(Continued)

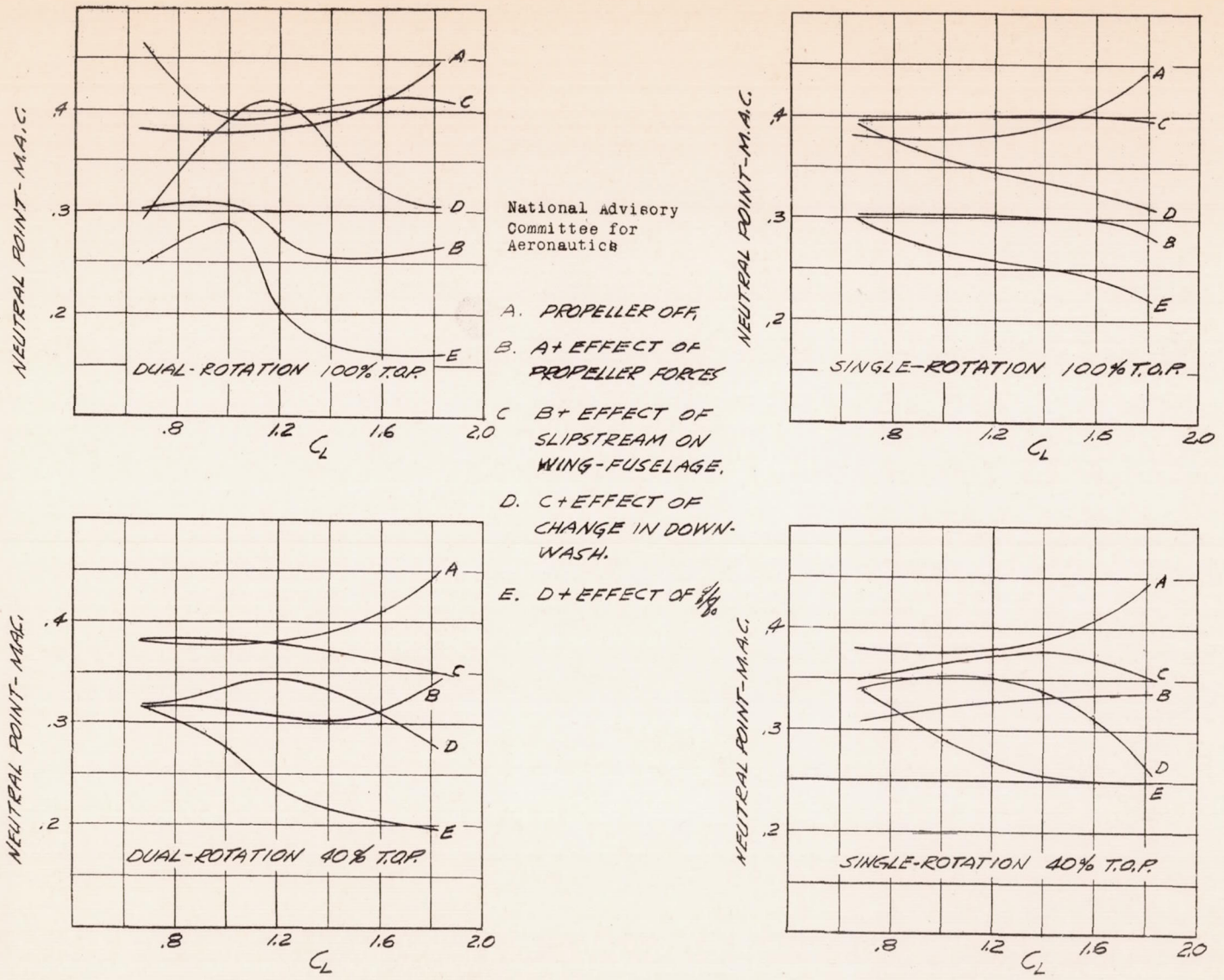

FIGURE 13.(CONCLUDED). SHIFT IN THE NEUTRAL POINT OF THE XSB2D-1 (C) CAUSED BY THE VARIOUS EFFECTS OF POWER. FLAPS DEFLECTED TO 38°.

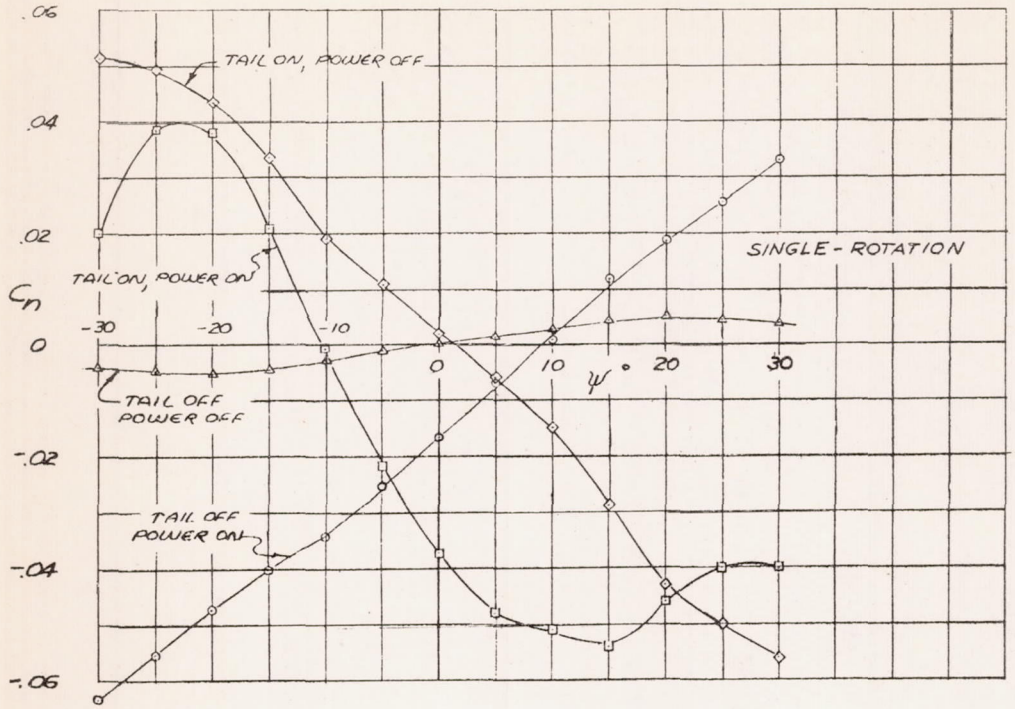

National Advisory Committee for Aeronautics

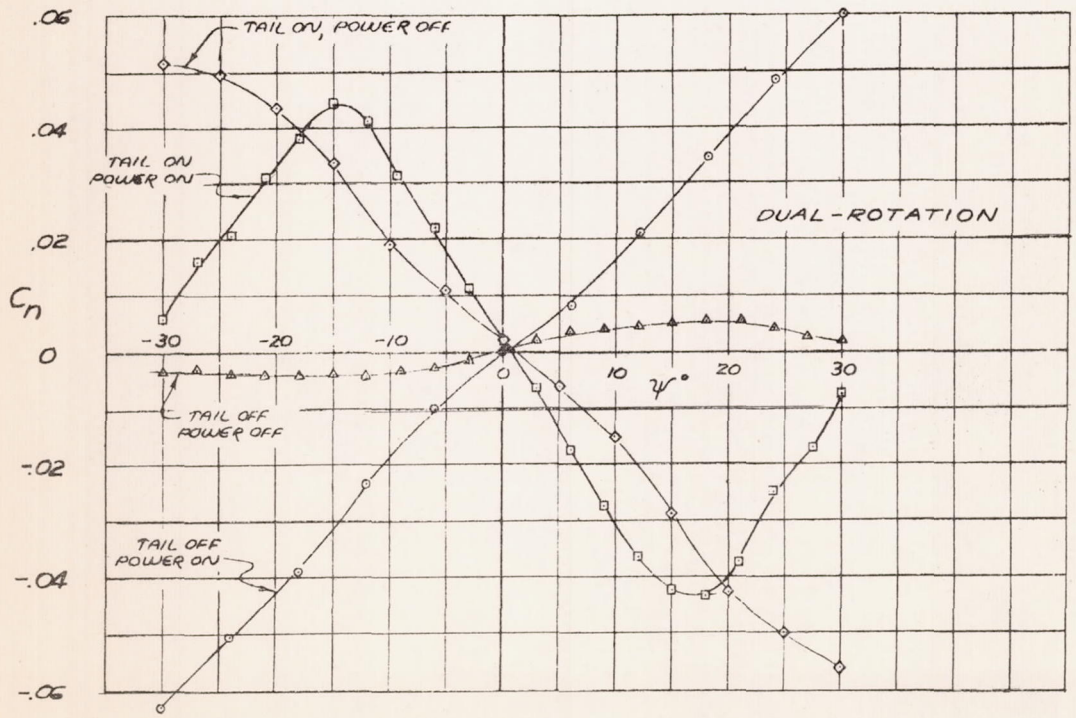

FIG. 14.- EFFECT OF POWER ON YAWING MOMENT VARIATION WITH ANGLE OF YAW OF THE XSB2D-1 MODEL WITH TAIL ON, AND WITH TAIL OFF. FLAPS 38° $\alpha_u = 7.6°$. $T_C = .81$

A-43

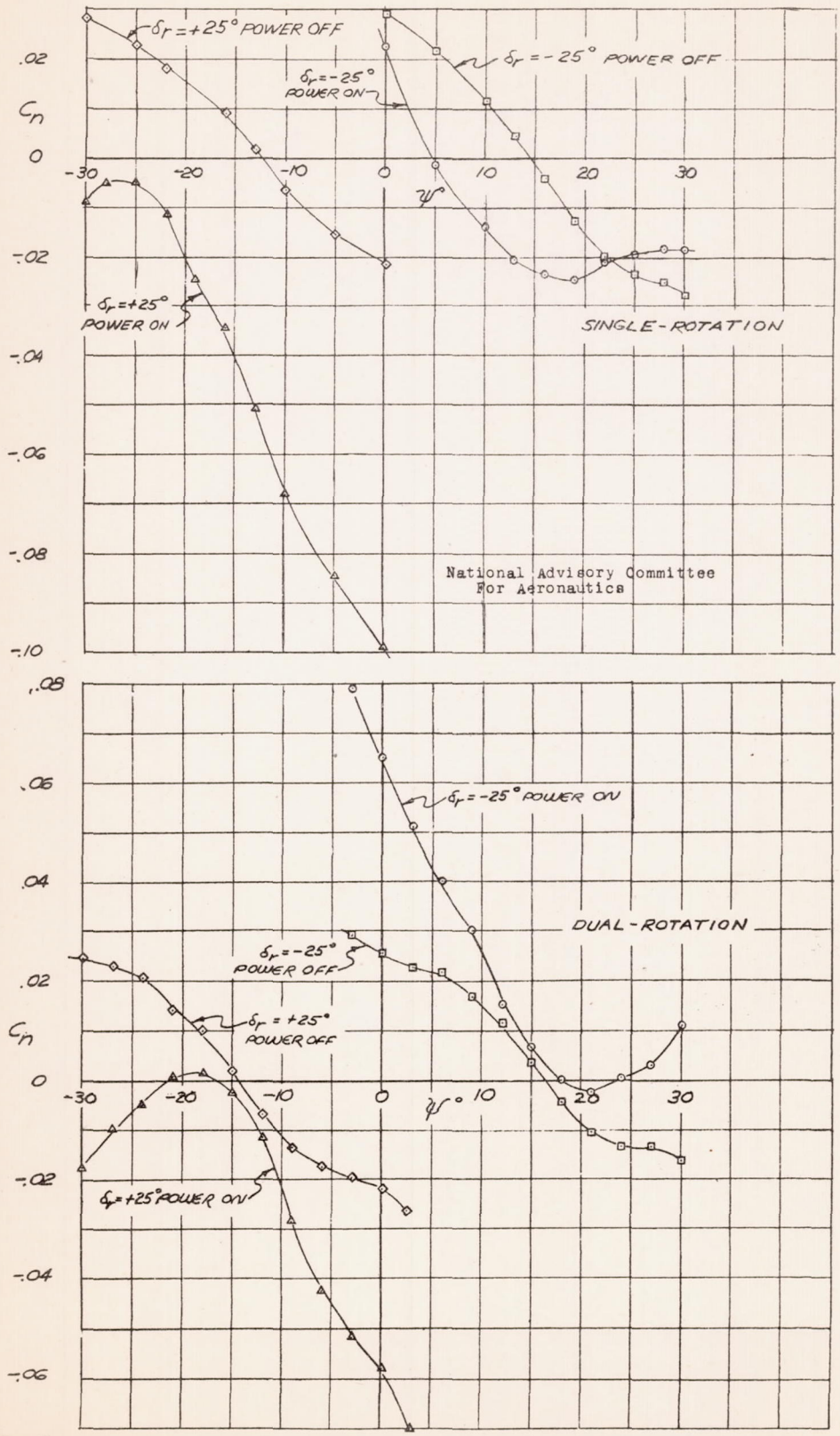

FIG. 15.- CHANGE IN EFFECTIVENESS OF RUDDER DUE TO POWER.
XSB2D-1 MODEL. FLAPS 38° α_u = 7.6. T_c = .81

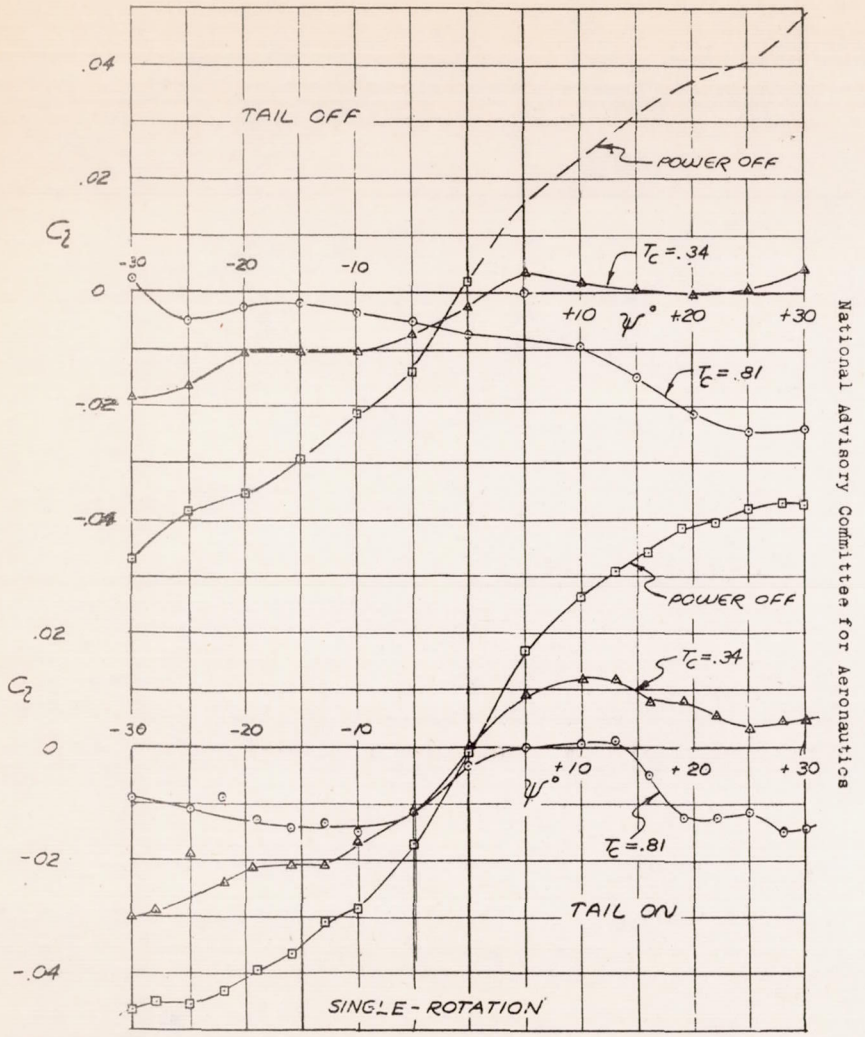

(a)

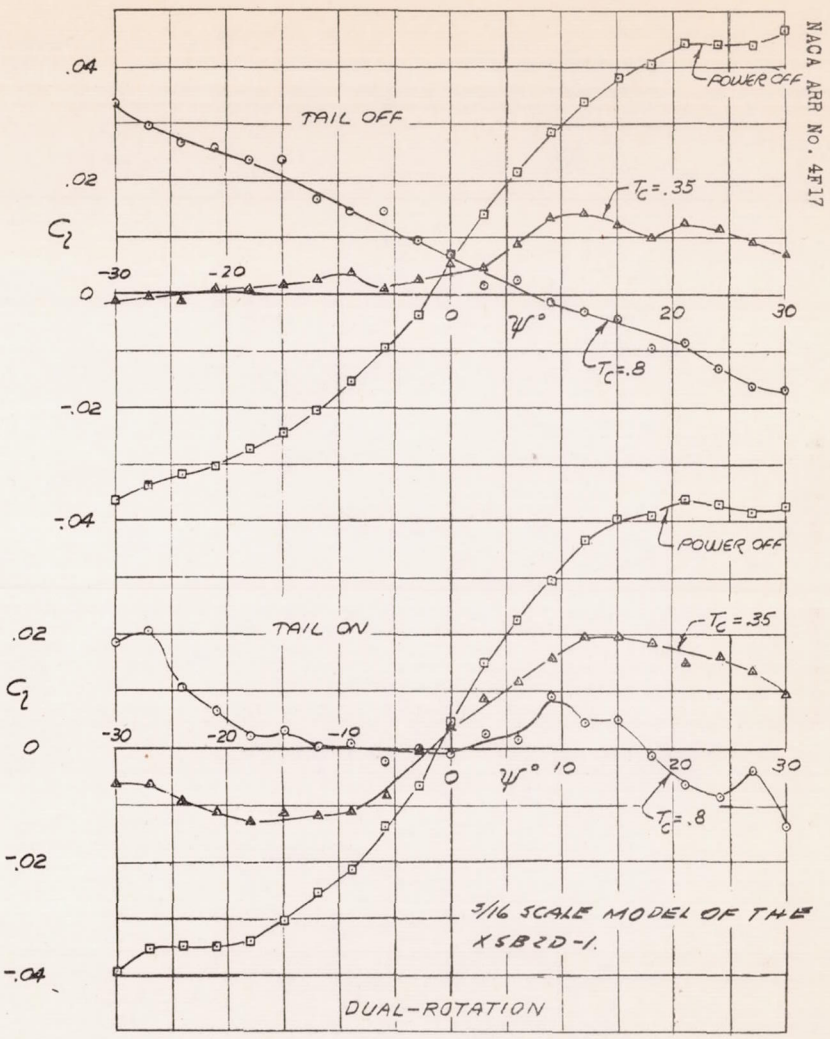

(b)

FIG. 16.- EFFECT OF POWER ON TAIL OFF AND TAIL ON VARIATION OF ROLLING MOMENT WITH YAW OF THE XSB2D-1 MODEL. FLAPS 38° α_w = 7.6°.

National Advisory Committee for Aeronautics

NACA ARR No. 4F17

FIG. 16

A-43

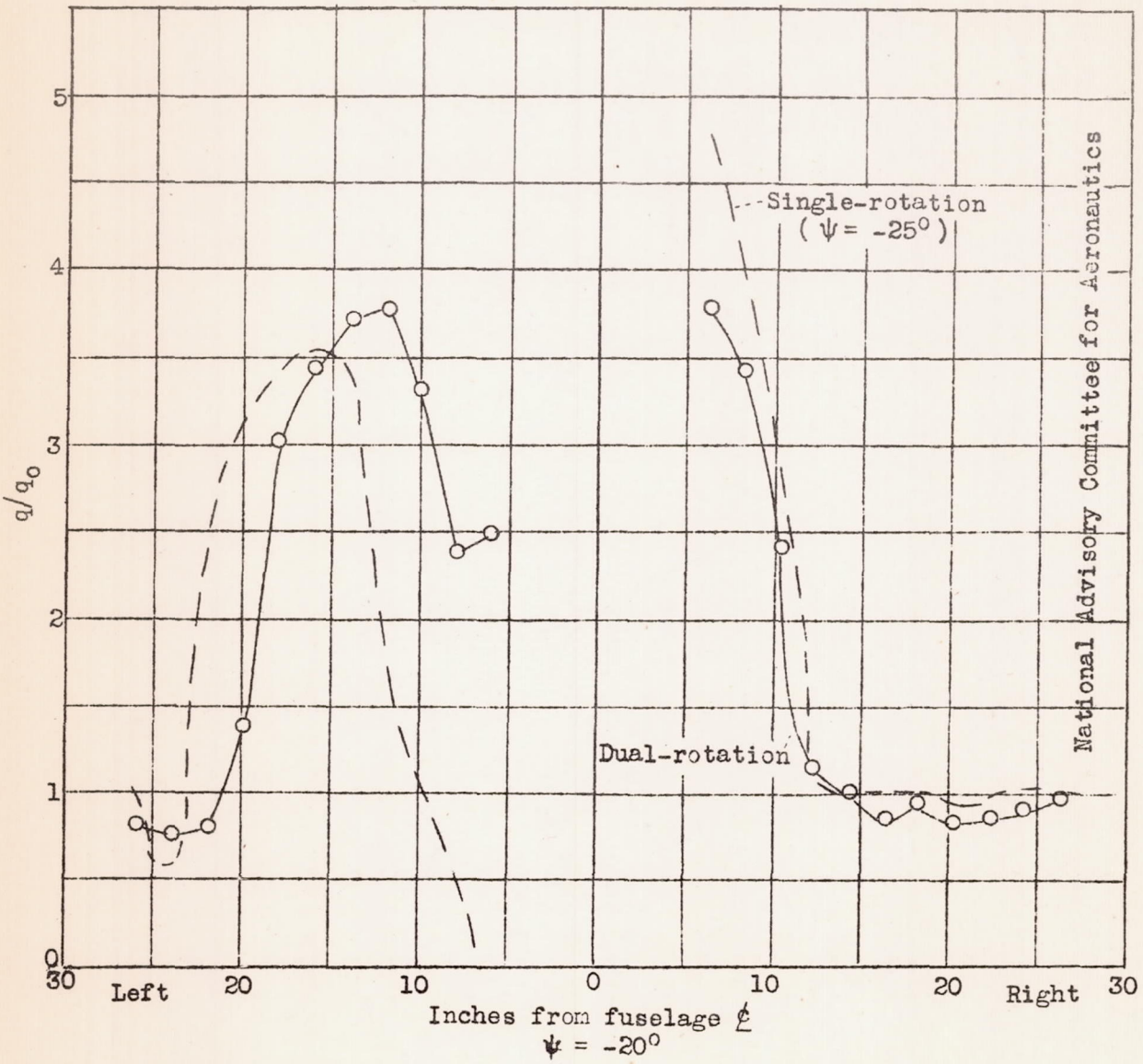

Figure 17(a to i).- Spanwise dynamic pressure variation based on total-head surveys at approximately the 25-percent-chord line of the XSB2D-1 model wing, four-blade propellers, blade angle of 21.6°, flaps 55°, 0° angle of attack, thrust coefficient (T_c) of 0.9.

A-43

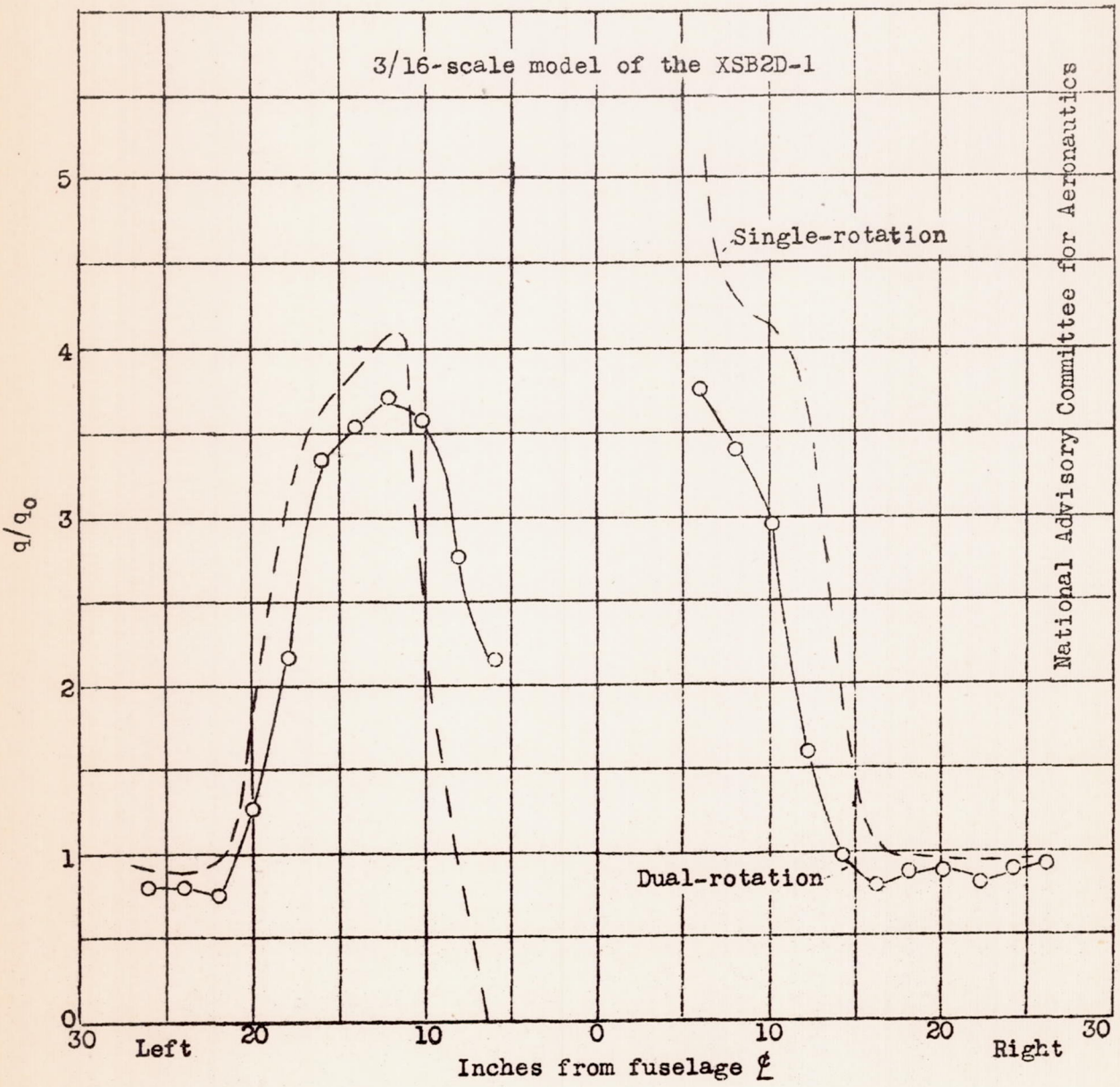

Figure 17b.- $\psi = -15^{\circ}$

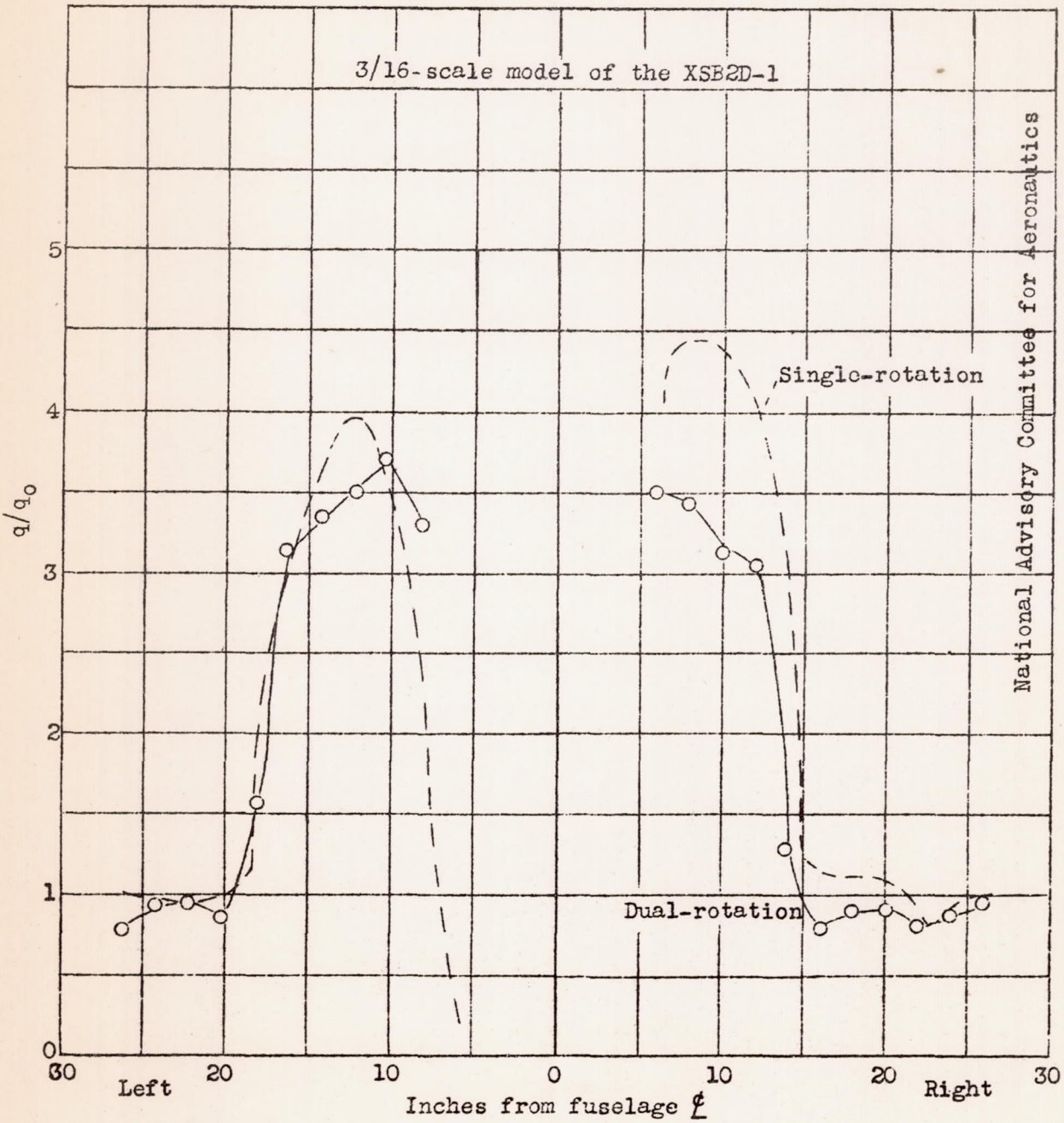

Figure 17c.- $\psi = -10^{\circ}$

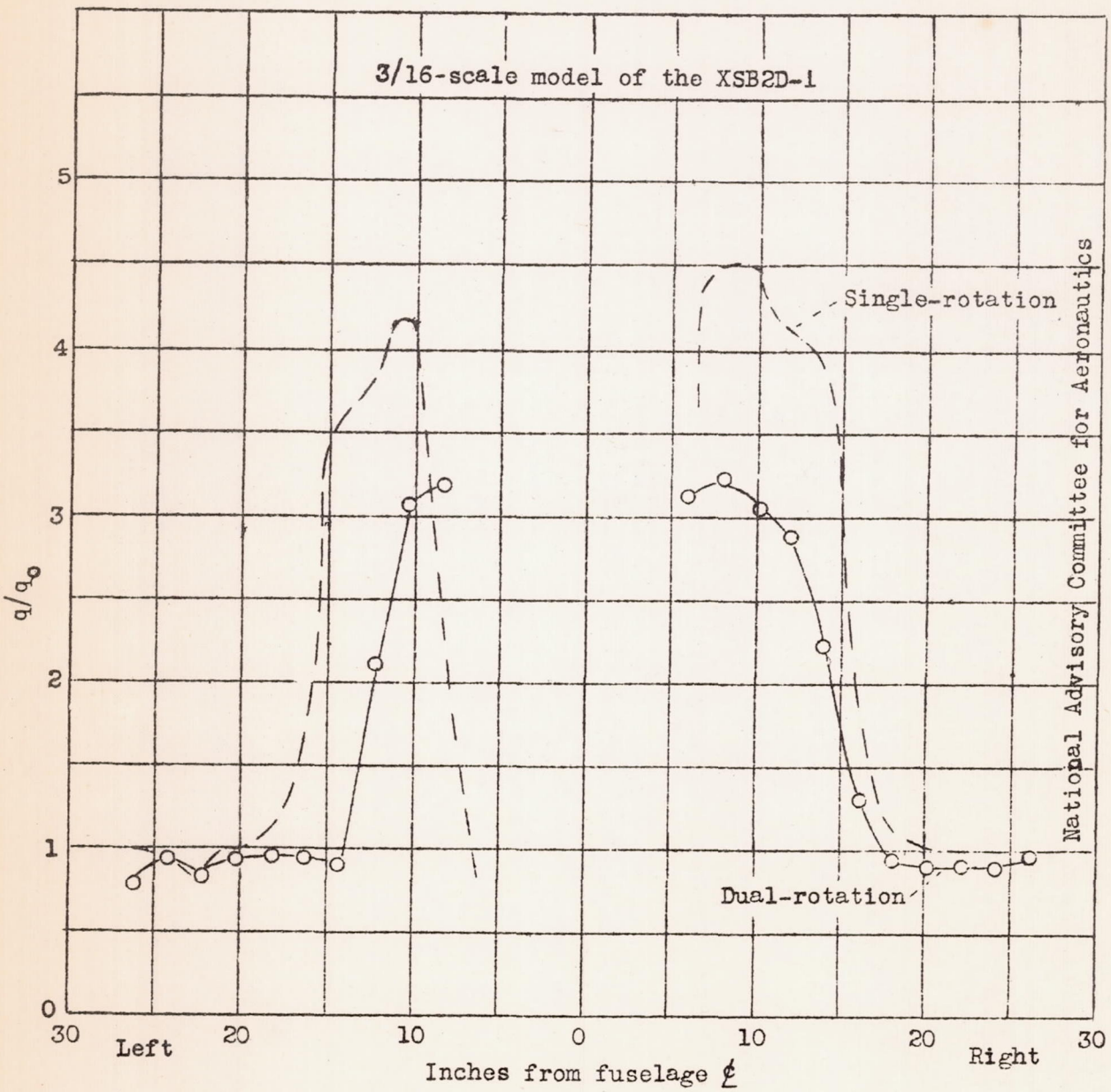

Figure 17d.- $\psi = -5^{\circ}$

A-43

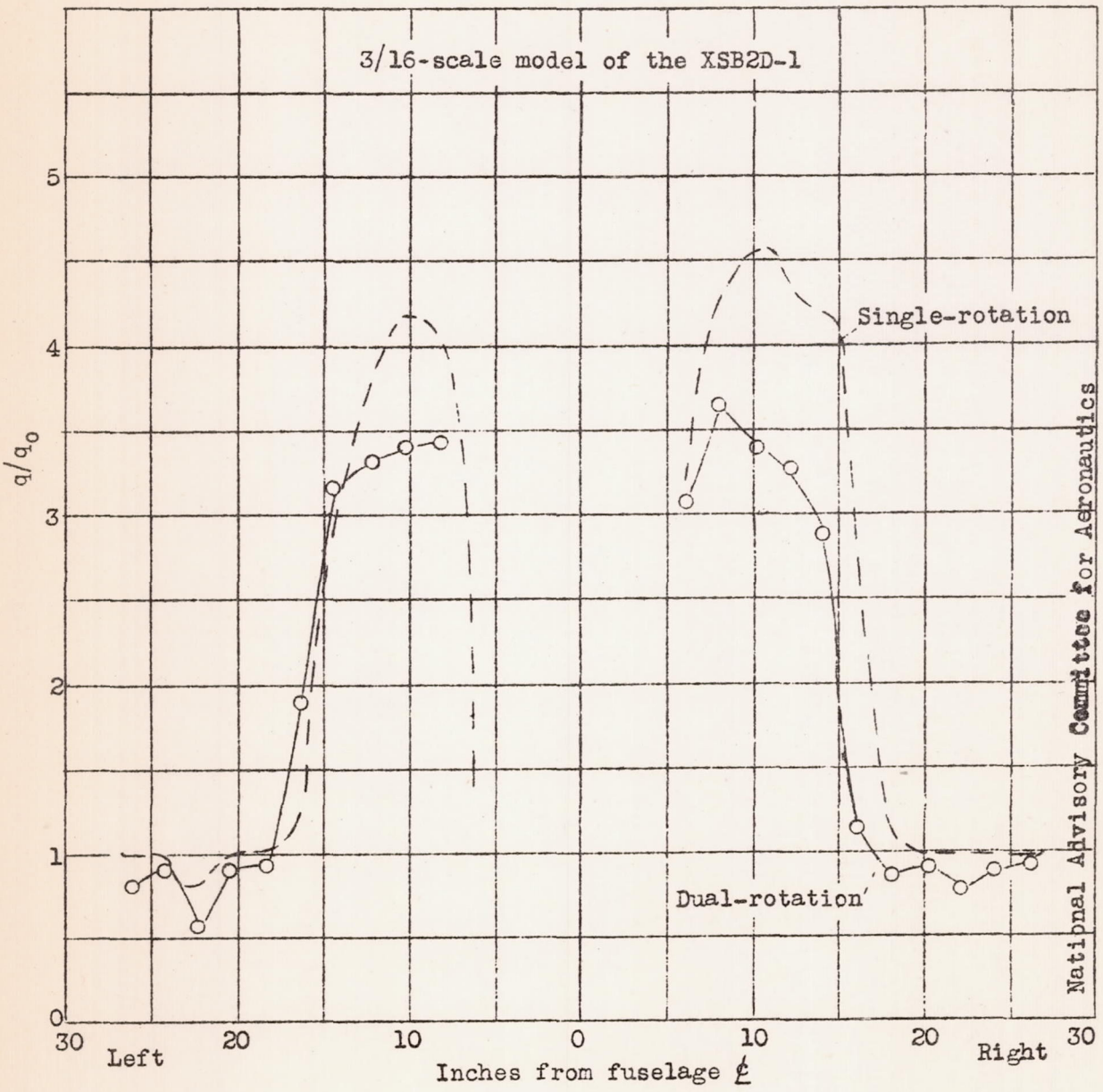

Figure 17e.- $\psi = 0°$

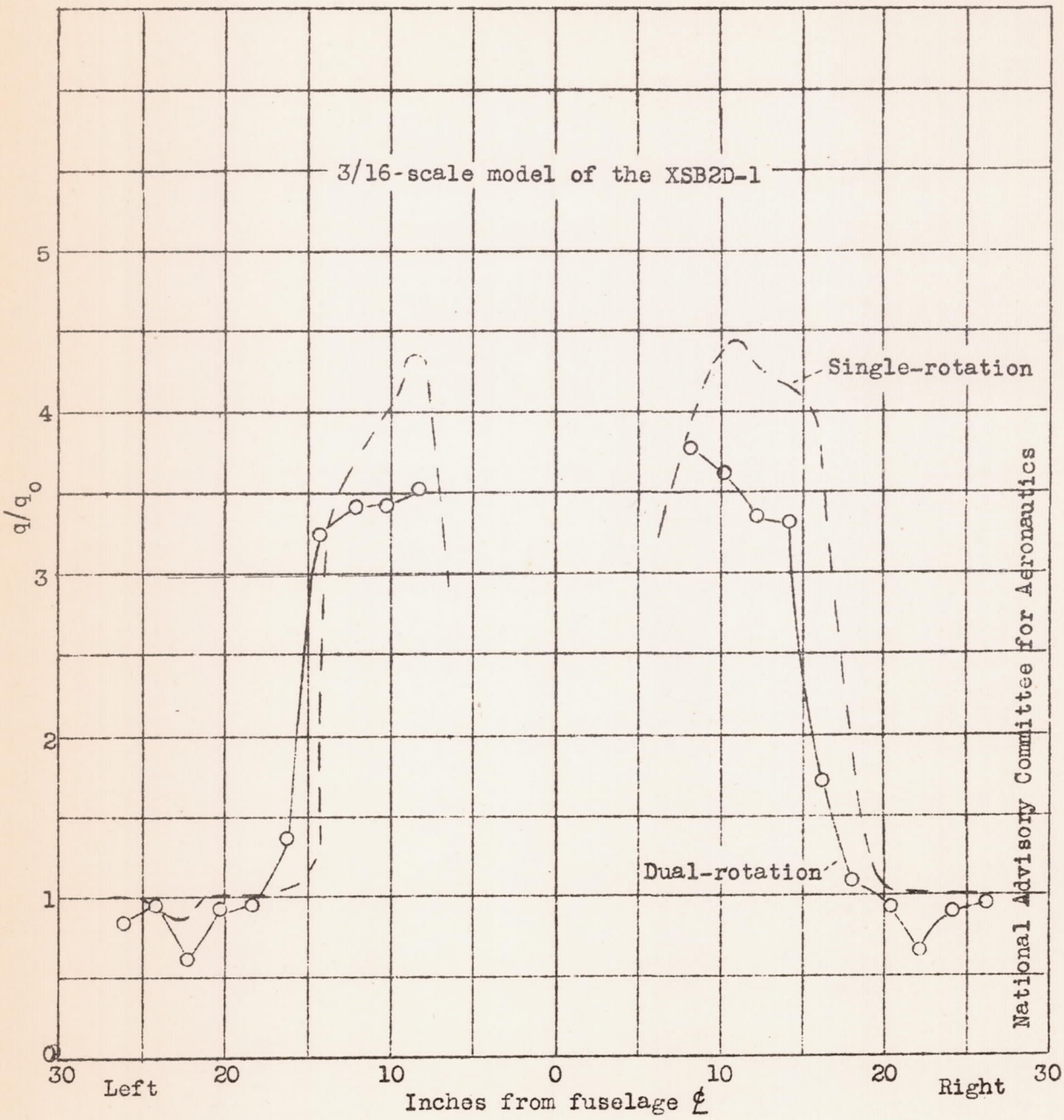

Figure 17f.- $\psi = .5^{\circ}$

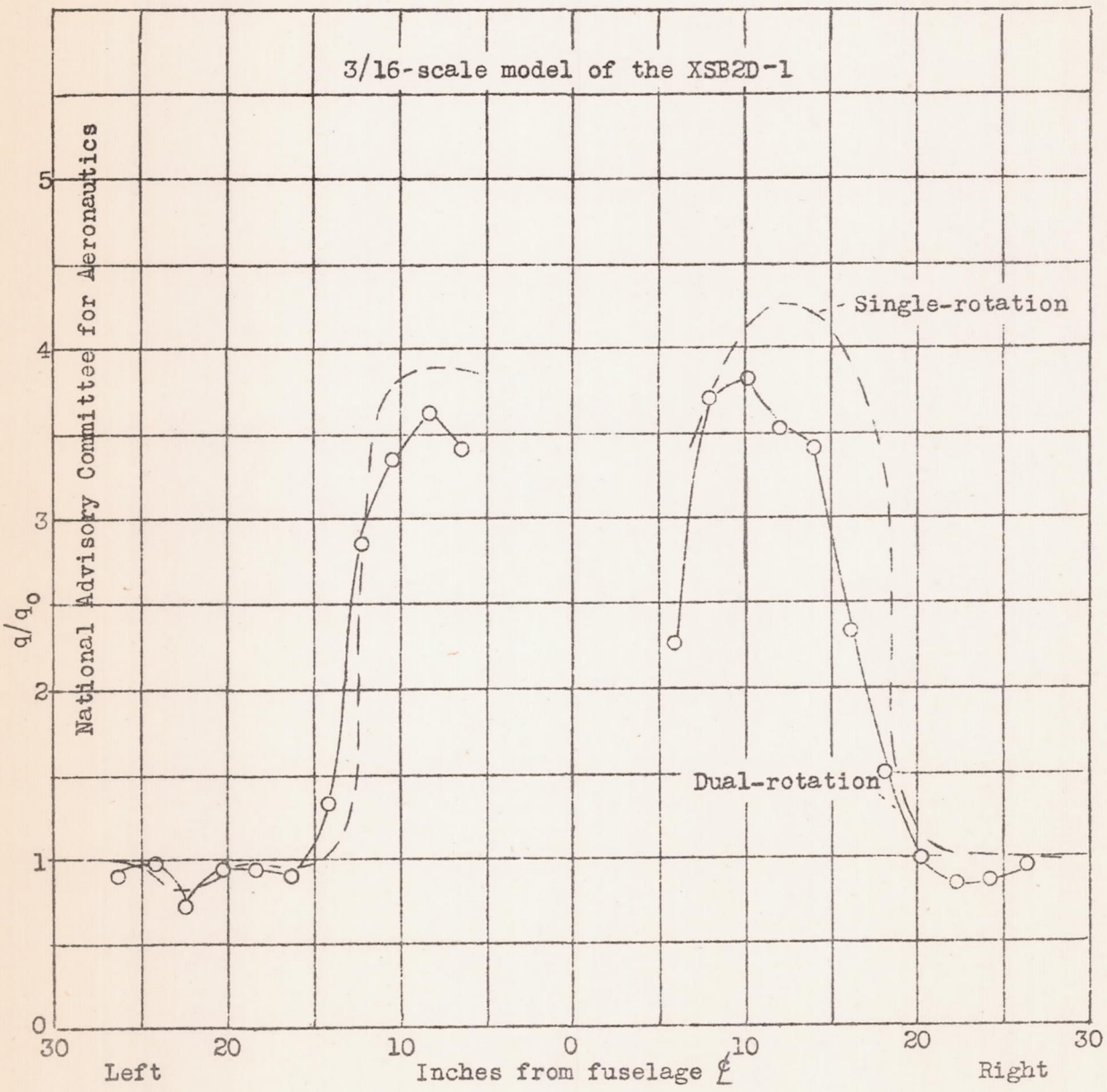

Figure 17g.- $\psi = +10^{\circ}$

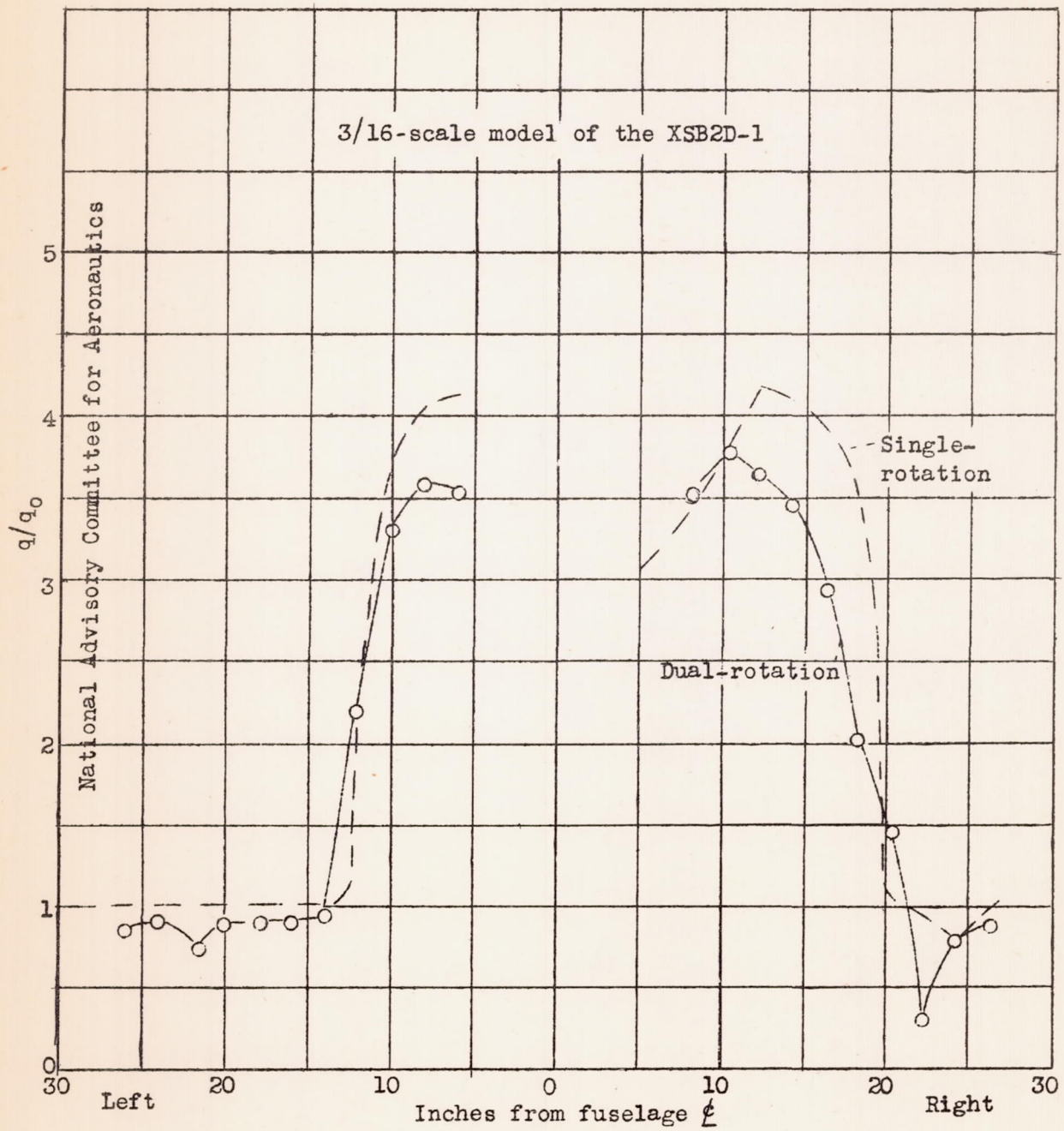

Figure 17h.- $\psi = 15^{\circ}$

A-43

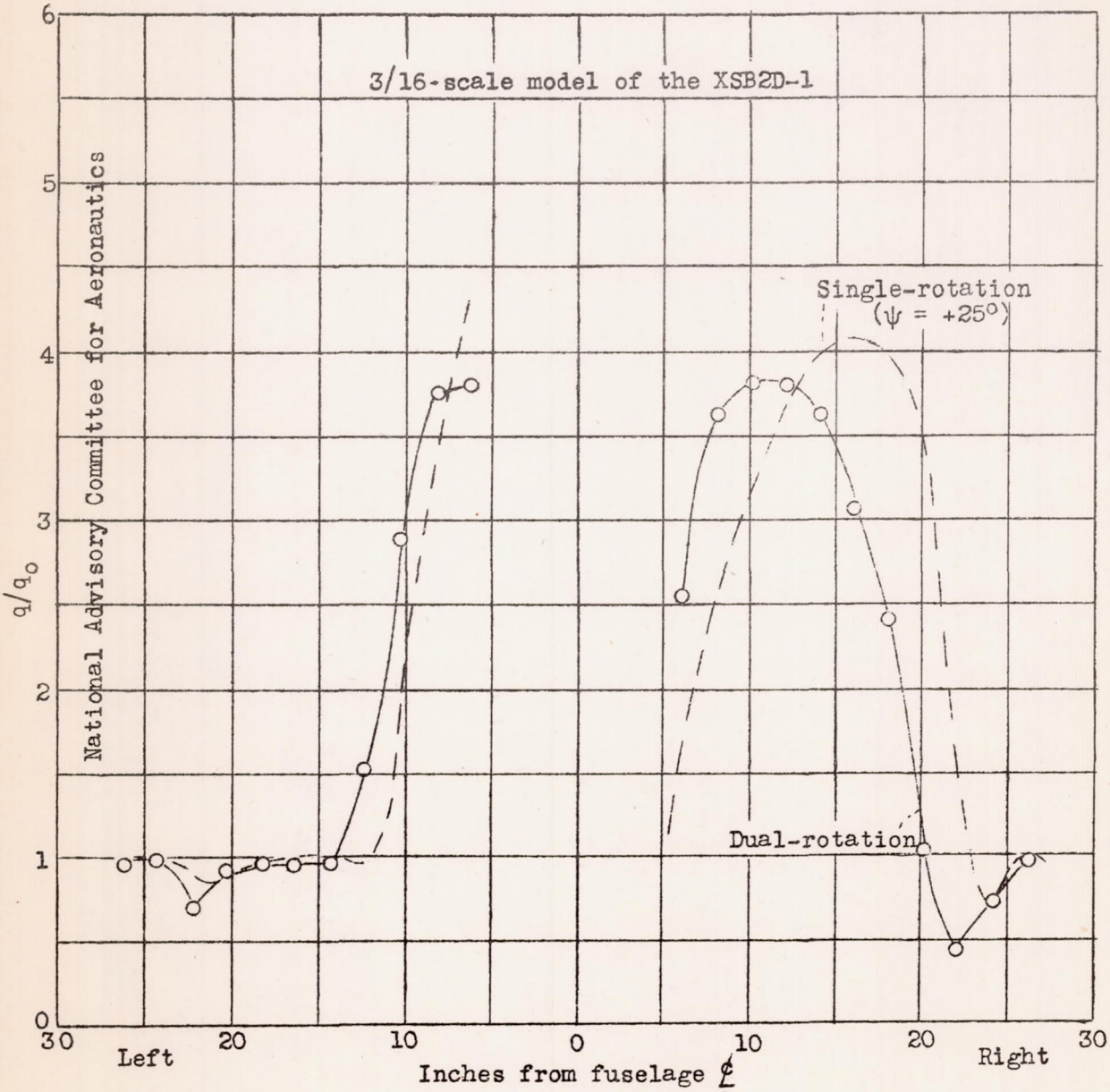

Figure 17i.- $\psi = -20^{\circ}$